DO-TH 2001/03
February 2001

Spin-Dependent Structure Functions of Real and Virtual Photons

M. Glück, E. Reya, C. Sieg

Universität Dortmund, Institut für Physik,
D-44221 Dortmund, Germany

Abstract

The implications of the positivity constraint, $|g_1^{\gamma(P^2)}(x,Q^2)| \leq F_1^{\gamma(P^2)}(x,Q^2)$, on the presently unknown spin–dependent structure function $g_1^{\gamma(P^2)}(x,Q^2)$ of real and virtual photons are studied at scales $Q^2 \gg P^2$ where longitudinally polarized photons dominate physically relevant cross sections. In particular it is shown how to implement the physical constraints of positivity and continuity at $P^2 = 0$ in NLO calculations which afford a nontrivial choice of suitable (DIS) factorization schemes related to g_1^γ and F_1^γ and appropriate boundary conditions for the polarized parton distributions of real and virtual photons. The predictions of two extreme 'maximal' and 'minimal' saturation scenarios are presented and compared with results obtained within the framework of a simple quark 'box' calculation expected to yield reasonable estimates in the not too small regions of x and P^2.

1 Introduction

The structure functions of photons with momentum p and virtuality $P^2 = -p^2$ probed at a scale $Q^2 \gtrsim 1$ GeV^2 and $Q^2 \gg P^2$, i.e. in the 'Bjorken limit', can be described in terms of photonic parton distributions. These spin–[in]dependent parton distributions of $\gamma(P^2)$, henceforth denoted by $\left[f^{\gamma(P^2)}(x,Q^2)\right]$ and $\Delta f^{\gamma(P^2)}(x,Q^2)$ with $f = q, \bar{q}, g$ and $q = u, d, s$, provide the dominant, lowest–twist, contributions to the structure functions $\left[F_{1,2}^{\gamma(P^2)}(x,Q^2)\right]$ and $g_1^{\gamma(P^2)}(x,Q^2)$ in [un]polarized deep elastic ep collisions.

One expects, of course, a unified description of real ($P^2 = 0$) and virtual ($P^2 \neq 0$) photons in the sense of continuity of all the physical predictions at $P^2 = 0$. It turns out, however, that the so–called 'direct' contribution to the structure functions due to the subprocess $\gamma^*(Q^2)\gamma(P^2) \to q\bar{q}$ which arises at the next–to–leading order (NLO) analysis of $F_{1,2}^{\gamma(P^2)}$ and $g_1^{\gamma(P^2)}$ is discontinuous at $P^2 = 0$, thus violating the basic continuity demand.

It was pointed out in [1] that the physically compelling continuity at $P^2 = 0$ is facilitated by treating the direct–photon contribution at $P^2 \neq 0$ to be the same as for a real on–shell ($P^2 = 0$) photon. As a logical consequence of this approach to the continuity demand it is mandatory to consider the direct contribution of the virtual photon to any deep inelastic scattering (DIS) process as if it was real. In [1] the consequences of this approach to spin–independent DIS processes were presented. The present paper extends this study to the spin–dependent DIS processes.

In Section 2 we present some consequences of our unified approach as reflected by the spin–dependent structure function $g_1^{\gamma(P^2)}(x,Q^2)$ characterizing the spin–dependent deep–inelastic inclusive $\gamma^*(Q^2)\gamma(P^2) \to$ hadrons scattering process accessible in longitudinally polarized e^+e^- annihilations. Here the various possible (input) boundary conditions for the polarized parton distributions and structure functions of longitudinally polarized real and virtual photons are discussed and presented together with their formal analytic solu-

tions of the inhomogeneous renormalization group (RG) Q^2–evolution equations. Various illustrative quantitative expectations are presented in Section 3. These QCD resummed RG–improved calculations are compared in Section 4 with the predictions of the standard non–resummed 'naive' quark–parton model (QPM) QED 'box' approach. In particular, the relevance of the polarized gluonic photon content, the typical RG–improved QCD ingredient, is studied within this context. Finally, our conclusions are summarized in Section 5.

2 $g_1^{\gamma(P^2)}(x,Q^2)$ and the associated parton distributions of polarized real and virtual photons

The flux of (longitudinally) polarized virtual photons produced by the the bremsstrahlung process of high energy electrons $e(k) \to e(k') + \gamma(p)$, $P^2 \equiv -p^2 = -(k'-k)^2$, at e^+e^- or ep colliders is given by [2]

$$\Delta f_{\gamma(P^2)/e}(y) = \frac{\alpha}{2\pi}\left[\frac{1-(1-y)^2}{y}\,\frac{1}{P^2} + \frac{2m_e^2 y^2}{P^4}\right] \tag{2.1}$$

where $y = E_\gamma/E_e$ and $\alpha \simeq 1/137$. The real ($P \simeq 0$) photons usually considered are those whose virtuality is in reality very small, i.e. of order $P^2_{\rm min} = \mathcal{O}(m_e^2)$ or, experimentally, at least $P^2 < 10^{-2}$ GeV^2 which is the case for the bulk of produced photons in untagged or antitagging experiments. On the other hand, a sizeable finite virtuality is achieved by tagging of the outgoing electron at the photon producing vertex $e \to e\gamma$. Whenever these virtual photons, with their virtuality being entirely taken care of by the flux factor in (2.1), are probed at a scale $Q^2 \gg P^2$ they may be considered as real photons, which means that cross sections of partonic subprocesses involving $\gamma(P^2)$ should be calculated as if $P^2 = 0$ (partly due to the suppression of any additional terms). Furthermore, the polarized parton distributions $\Delta f^{\gamma(P^2)}(x,Q^2)$ of the virtual photon obey the same Q^2 evolution, i.e. renormalization group (RG), equations as the real photon $\gamma \equiv \gamma(P^2=0)$ distributions $\Delta f^{\gamma}(x,Q^2)$ and the only difference between them resides in the different

boundary conditions. This concept is similar to the one suggested and developed in [1] for unpolarized photons which, as emphasized in the Introduction, follows from the basic continuity demand at $P^2 = 0$.

Following the situation of protons [3] and unpolarized photons [1], the structure function of polarized photons $g_1^{\gamma(P^2)}(x,Q^2)$ will be decomposed into $g_{1,\ell}^{\gamma(P^2)}$ due to the light (massless) u,d,s partons, and $g_{1,h}^{\gamma(P^2)}$ due to the heavy $h = c,b,\ldots$ quarks whose contributions are calculated in fixed order of perturbation theory which are known and unproblematic due to the finite $m_h \neq 0$ (we shall come back to this point at the end of this Section). The main issue of this paper resides of course in $g_{1,\ell}^{\gamma(P^2)}$ which, up to NLO($\overline{\rm MS}$), is given by the following expression:

$$\begin{aligned} g_{1,\ell}^{\gamma(P^2)}(x,Q^2) &= \frac{1}{2}\sum_{q=u,d,s} e_q^2 \left\{ \Delta q^{\gamma(P^2)}(x,Q^2) + \Delta\bar{q}^{\,\gamma(P^2)}(x,Q^2) + \frac{\alpha_s(Q^2)}{2\pi} \right. \\ &\left. \times \left[\Delta C_q \otimes \Delta(q+\bar{q})^{\gamma(P^2)} + 2\Delta C_g \otimes \Delta g^{\gamma(P^2)} \right] + e_q^2 \frac{\alpha}{\pi} \Delta C_\gamma(x) \right\} \quad (2.2) \end{aligned}$$

where $\otimes$ denotes the usual convolution integral. Here, $\Delta\bar{q}^{\,\gamma(P^2)} = \Delta q^{\gamma(P^2)}$ and $\Delta g^{\gamma(P^2)}$ provide the so–called 'resolved' contribution of $\gamma(P^2)$ to $g_{1,\ell}^{\gamma(P^2)}$ with the usual hadronic polarized Wilson coefficient functions in the conventional $\overline{\rm MS}$ factorization scheme given by [4, 5]

$$\begin{aligned} \Delta C_q(x) &= \frac{4}{3}\left[(1+x^2)\left(\frac{\ln(1-x)}{1-x}\right)_+ - \frac{3}{2}\frac{1}{(1-x)_+} - \frac{1+x^2}{1-x}\ln x + 2 + x \right. \\ &\left. - \left(\frac{9}{2} + \frac{\pi^2}{3}\right)\delta(1-x) \right] \\ \Delta C_g(x) &= \frac{1}{2}\left[(2x-1)\left(\ln\frac{1-x}{x} - 1\right) + 2(1-x) \right] . \quad (2.3) \end{aligned}$$

The aforementioned 'direct' contribution is provided by the $\Delta C_\gamma(x)$ term in (2.2) which has to be calculated for <u>real</u> photons $\gamma \equiv \gamma(P^2 = 0)$, as follows from the continuity condition, in the polarized 'box' subprocess $\gamma^*(Q^2)\gamma \to q\bar{q}$. Thus ΔC_γ can be easily obtained from ΔC_g in (2.3) which is also derived for a massless on–shell gluon in the

polarized subprocess $\gamma^*(Q^2)g \to q\bar{q}$:

$$\Delta C_\gamma(x) = \frac{3}{(1/2)}\Delta C_g(x) = 3\left[(2x-1)\left(\ln\frac{1-x}{x} - 1\right) + 2(1-x)\right] . \tag{2.4}$$

The NLO coefficient functions $\Delta C_{q,g,\gamma}$ are obviously factorization scheme dependent and we shall follow the traditional choice [6], motivated by the perturbative stability of unpolarized photon structure functions, where $\Delta C_{q,g}$ are considered in the $\overline{\rm MS}$ scheme while the destabilizing ΔC_γ term in (2.2), as given by (2.4), is entirely absorbed [1, 6, 7] into the $\overline{\rm MS}$ (anti)quark densities in (2.2) as implied by the so-called 'polarized DIS$_\gamma$' factorization scheme, to be denoted by DIS$_{\Delta\gamma}$:

$$\begin{aligned} (\Delta q + \Delta\bar{q})^{\gamma(P^2)}_{\rm DIS_{\Delta\gamma}} &= (\Delta q + \Delta\bar{q})^{\gamma(P^2)} + e_q^2\,\frac{\alpha}{\pi}\,\Delta C_\gamma(x) \\ \Delta g^{\gamma(P^2)}_{\rm DIS_{\Delta\gamma}} &= \Delta g^{\gamma(P^2)} . \end{aligned} \tag{2.5}$$

This redefinition of parton distributions implies that the polarized NLO($\overline{\rm MS}$) splitting functions $\Delta k^{(1)}_{q,g}(x)$ of the photon into quarks and gluons, appearing in inhomogeneous NLO RG Q^2–evolution equations [7] for $\Delta f^{\gamma(P^2)}(x,Q^2)$, have correspondingly to be transformed according to [6, 8]

$$\begin{aligned} \Delta k^{(1)}_q|_{\rm DIS_{\Delta\gamma}} &= \Delta k^{(1)}_q - e_q^2\,\Delta P^{(0)}_{qq} \otimes \Delta C_\gamma \\ \Delta k^{(1)}_g|_{\rm DIS_{\Delta\gamma}} &= \Delta k^{(1)}_g - 2\sum_q e_q^2\,\Delta P^{(0)}_{gq} \otimes \Delta C_\gamma \end{aligned} \tag{2.6}$$

where [7]

$$\begin{aligned} \Delta k^{(1)}_q(x) &= \frac{1}{2}\,3e_q^2\,\frac{4}{3}\Big\{-9\ln x + 8(1-x)\,\ln(1-x) + 27x - 22 \\ &\quad +(2x-1)\left[\ln^2 x + 2\ln^2(1-x) - 4\ln x\ln(1-x) - \frac{2}{3}\pi^2\right]\Big\} \\ \Delta k^{(1)}_g(x) &= 3\sum_q e_q^2\,\frac{4}{3}\left\{-2(1+x)\,\ln^2 x + 2(x-5)\,\ln x - 10(1-x)\right\} \end{aligned} \tag{2.7}$$

with $\Delta k^{(1)}_q$ referring to each single (anti)quark flavor. The polarized LO splitting functions are given by $\Delta P^{(0)}_{qq} = \frac{4}{3}\left(\frac{1+x^2}{1-x}\right)_+$ and $\Delta P^{(0)}_{gq} = \frac{4}{3}(2-x)$. The NLO expression for $g^{\gamma(P^2)}_{1,\ell}$ in

the $\mathrm{DIS}_{\Delta\gamma}$ scheme is thus given by (2.2) with $\Delta C_\gamma(x)$ being dropped. Since from now on we shall exclusively work in this DIS_γ scheme, we skip the label '$\mathrm{DIS}_{\Delta\gamma}$' on all our subsequent parton distributions and splitting functions. The leading order (LO) expression for $g_{1,\ell}^{\gamma(P^2)}$ is obviously obtained from eq. (2.2) by simply setting $\Delta C_{q,g,\gamma} = 0$.

The general solution of the inhomogeneous evolution equations [7] for $\Delta f^{\gamma(P^2)}(x,Q^2)$ may be written as

$$\Delta f^{\gamma(P^2)}(x,Q^2) = \Delta f_{p\ell}^{\gamma(P^2)}(x,Q^2) + \Delta f_{\mathrm{had}}^{\gamma(P^2)}(x,Q^2) \tag{2.8}$$

and similarly for $g_{1,\ell}^{\gamma(P^2)}(x,Q^2)$ in (2.2). The nonhadronic 'pointlike' component $\Delta f_{p\ell}^{\gamma(P^2)}$ evolves according to the full inhomogeneous evolution equations subject to the boundary condition

$$\Delta f_{p\ell}^{\gamma(P^2)}(x,\tilde{P}^2) = 0\,, \qquad \tilde{P}^2 = \max\,(P^2,\mu^2) \tag{2.9}$$

with μ being some appropriately chosen resolution scale taken here, in the spirit of the radiative parton model [3], to be [1, 3] $\mu^2_{\mathrm{NLO(LO)}} = 0.40\ (0.26)\ \mathrm{GeV}^2$. The 'hadronic' component in (2.8) represents the solution to the conventional homogeneous evolution equations where the photon splitting functions $\Delta k_{q,g}^{(0,1)}$ are dropped. Following refs. [7, 9] we shall study two extreme scenarios for $\Delta f_{\mathrm{had}}^{\gamma(P^2)}(x,Q^2)$:

(i) a 'maximal' scenario corresponding to a NLO input

$$\Delta f_{\mathrm{had}}^{\gamma(P^2)}(x,\tilde{P}^2)) = \eta(P^2)\, f_{\mathrm{had}}^{\gamma}(x,\tilde{P}^2)_{\mathrm{DIS}_{\gamma,1}} \tag{2.10}$$

where $\eta(P^2) = (1 + P^2/m_\rho^2)^{-2}$ is a dipole suppression factor with $m_\rho^2 = 0.59\ \mathrm{GeV}^2$, and in LO the unpolarized photonic parton distributions $f_{\mathrm{had}}^{\gamma}(x,\tilde{P}^2)_{\mathrm{LO}}$ refer to the common LO (input) densities as obtained, for example, in [1];

(ii) a 'minimal' scenario corresponding to a NLO input [10]

$$\begin{aligned}
\Delta q_{\rm had}^{\gamma(P^2)}(x,\tilde{P}^2) &= \eta(P^2) e_q^2 \frac{\alpha}{2\pi}\left[C_{\gamma,1}(x) - C_{\gamma,2}(x)\right] \\
&= \eta(P^2) e_q^2 \frac{\alpha}{2\pi}\left[-12x(1-x)\right] \\
\Delta g_{\rm had}^{\gamma(P^2)}(x,\tilde{P}^2) &= 0\,, \qquad (2.11)
\end{aligned}$$

whereas in LO $\Delta q_{\rm had}^{\gamma}(x,\tilde{P}^2)$ also vanishes, due to the absence of the (unpolarized) NLO coefficient functions $C_{\gamma,i}$, and thus the input $\Delta f^{\gamma(P^2)}(x,\tilde{P}^2)_{\rm LO} = 0$ coincides with the 'pointlike' LO solution for $\Delta f^{\gamma(P^2)}(x,Q^2)_{\rm LO}$ in (2.8) with [1] $\mu^2_{\rm LO} = 0.26$ GeV^2. Thus this 'minimal' scenario constitutes a genuinely lowest, but possibly unrealistic, limit for the expected parton distributions of a longitudinally polarized photon.

It should be noticed that the unpolarized NLO inputs in (2.10) and (2.11) refer to the so–called DIS$_{\gamma,1}$ factorization scheme [10] related to F_1^γ, rather than to F_2^γ, in order to comply with the fundamental positivity constraint $|A_1^{\gamma(P^2)}| \equiv |g_1^{\gamma(P^2)}/F_1^{\gamma(P^2)}| \leq 1$, to which we shall turn in more detail in the next Section. The unpolarized parton distributions in the DIS$_{\gamma,1}$ factorization scheme required in (2.10) can be easily derived from the ones in the DIS$_\gamma$ scheme [1, 6, 8], as obtained from an analysis [1] of the data on F_2^γ, via [10]

$$\begin{aligned}
q^\gamma(x,Q^2)_{\rm DIS_{\gamma,1}} &= q^\gamma(x,Q^2)_{\rm DIS_\gamma} - e_q^2 \frac{\alpha}{2\pi} 12x(1-x) \\
g^\gamma(x,Q^2)_{\rm DIS_{\gamma,1}} &= g^\gamma(x,Q^2)_{\rm DIS_\gamma}\,. \qquad (2.12)
\end{aligned}$$

These boundary conditions are dictated, as in [1], by the continuity of $\Delta f^{\gamma(P^2)}(x,Q^2)$ at $P^2 = 0$. The hadronic vector–meson–dominance (VMD) oriented input distributions of the unpolarized real photon $f_{\rm had}^\gamma(x,Q^2)$ in (2.10) will also be taken from [1] for reasons of consistency with the positivity constraint. These scenarios will be considered below for our quantitative analyses.

It should be mentioned that our above boundary conditions for the hadronic input in NLO differ substantially from those considered by Sasaki and Uematsu [11, 12] who consider only the kinematical region $\Lambda^2 \ll P^2 \ll Q^2$ in contrast to our analysis addressing

the full kinematical region $0 \leq P^2 \ll Q^2$ and the ensuing continuity constraints at $P^2 = 0$. More specifically, Sasaki and Uematsu [11, 12] consider on the contrary the perturbatively calculable doubly–virtual polarized box $\gamma^*(Q^2)\gamma(P^2) \to q\bar{q}$, following the original treatment of the parton structure of the unpolarized virtual photon [13], and thus adopt for $\Delta f^{\gamma(P2)}_{\rm had,NLO}$ the following boundary condition at $Q^2 = P^2$ in the DIS$_\gamma$ factorization scheme:

$$\begin{aligned} \Delta q^{\gamma(P^2)}_{\rm had,NLO}(x, Q^2 = P^2) &= \Delta \bar{q}^{\gamma(P2)}_{\rm had,NLO}(x, Q^2 = P^2) \\ &= 3e_q^2 \, \frac{\alpha}{2\pi} \, (2x-1) \left(\ln \frac{1}{x^2} - 2 \right) \\ \Delta g^{\gamma(P^2)}_{\rm had,NLO}(x, Q^2 = P^2) &= 0 \, . \end{aligned} \tag{2.13}$$

Due to the nonvanishing virtuality ($P^2 \neq 0$) of the target photon, these results obviously cannot be related anymore, as in (2.4), to the one of a massless initial on–shell gluon in (2.3). Apart from exluding the polarized real ($P^2 = 0$) photon within this approach, the input in (2.13) is problematic on its own since kinematically x is restrained to $x \leq \frac{1}{2}$ at $Q^2 = P^2$ due to $0 \leq x \leq (1 + P^2/Q^2)^{-1}$. This latter problem is also faced in the treatment of the partonic structure of a virtual unpolarized photon as suggested originally in [14]. (The LO boundary conditions are, in contrast to (2.13), obviously given by $\Delta f^{\gamma(P^2)}_{\rm had,LO}(x, Q^2 = P^2) = 0$.) In view of $P^2 \gg \Lambda^2$ it is tacitly assumed in [11, 12] that the hadronic VMD input, eq. (2.10), is negligible. One can, however, also implement a smooth transition to $P^2 = 0$ in this approach by multiplying the r.h.s. of (2.13) by, say [15], $\zeta(P^2) = P^2/(P^2 + Q_0^2)$ where $Q_0^2 \simeq 1$ GeV^2, as derived from DIS ep structure functions, and adding to this part also the VMD hadronic component in (2.10). Alternatively a smooth transition to $P^2 = 0$ may be achieved by multiplying the r.h.s. of (2.13) by $[1 - \eta(P^2)]$ with $\eta(P^2)$ as in (2.10), as has been originally suggested for the unpolarized virtual photon [14].

Having fixed the boundary (input) conditions, we turn now to the inhomogeneous RG Q^2–evolution equations which are formally very similar to the ones of an unpolarized

real photon [6, 8], replacing the spin–independent splitting functions everywhere by their spin–dependent counterparts [7]. Their LO and NLO solutions can be given analytically for the Mellin n–moments of $\Delta f^{\gamma(P^2)}(x,Q^2)$ in (2.8):

$$\begin{aligned}\Delta f^{\gamma(P^2),n}(Q^2) &\equiv \int_0^1 dx\, x^{n-1} \Delta f^{\gamma(P^2)}(x,Q^2) \\ &= \Delta f_{p\ell}^{\gamma(P^2),n}(Q^2) + \Delta f_{\rm had}^{\gamma(P^2),n}(Q^2)\,. \end{aligned} \tag{2.14}$$

The 'pointlike' solution, which vanishes at the input scale $Q^2 = \tilde{P}^2$ in (2.9), is driven by the LO and NLO pointlike photon splitting functions $\Delta k_{q,g}^{(0,1)}$ appearing in the inhomogeneous evolution equations, while $\Delta f_{\rm had}^{\gamma(P^2)}$ depends on the hadronic input in (2.10) and evolves according to the standard homogeneous evolution equations. The flavor–singlet solutions for $f = 3$ flavors, i.e. $Q^2 \equiv Q_3^2 \leq m_c^2$, are given by

$$\begin{aligned}\begin{pmatrix} \Delta\Sigma_{p\ell}^{\gamma(P^2),n}(Q_3^2) \\ \Delta g_{p\ell}^{\gamma(P^2),n}(Q_3^2) \end{pmatrix} &= \frac{4\pi}{\alpha_s^{(3)}(Q_3^2)} \left(1 + \frac{\alpha_s^{(3)}(Q_3^2)}{2\pi} \Delta\hat{U}\right) \left[1 - L_3^{1-\frac{2}{\beta_0^{(3)}}\Delta\hat{P}^{(0)n}}\right] \\ &\times \frac{1}{1 - \frac{2}{\beta_0^{(3)}}\Delta\hat{P}^{(0)n}} \frac{\alpha}{2\pi\beta_0^{(3)}} \Delta\vec{k}^{\,(0)n} + \left[1 - L_3^{-\frac{2}{\beta_0^{(3)}}\Delta\hat{P}^{(0)n}}\right] \\ &\times \frac{1}{-\Delta\hat{P}^{(0)n}} \frac{\alpha}{2\pi} \left(\Delta\vec{k}^{(1)n} - \frac{\beta_1^{(3)}}{2\beta_0^{(3)}} \Delta\vec{k}^{(0)n} - \Delta\hat{U}\Delta\vec{k}^{(0)n}\right) \end{aligned} \tag{2.15}$$

$$\begin{aligned}\begin{pmatrix} \Delta\Sigma_{\rm had}^{\gamma(P^2),n}(Q_3^2) \\ \Delta g_{\rm had}^{\gamma(P^2),n}(Q_3^2) \end{pmatrix} &= \left[L_3^{-\frac{2}{\beta_0^{(3)}}\Delta\hat{P}^{(0)n}} + \frac{\alpha_s^{(3)}(Q_3^2)}{2\pi} \Delta\hat{U} L_3^{-\frac{2}{\beta_0^{(3)}}\Delta\hat{P}^{(0)n}} \right. \\ &\left. - \frac{\alpha_s^{(3)}(\tilde{P}^2)}{2\pi} L_3^{-\frac{2}{\beta_0^{(3)}}\Delta\hat{P}^{(0)n}} \Delta\hat{U}\right] \begin{pmatrix} \Delta\Sigma_{\rm had}^{\gamma(P^2),n}(\tilde{P}^2) \\ \Delta g_{\rm had}^{\gamma(P^2),n}(\tilde{P}^2) \end{pmatrix} \end{aligned} \tag{2.16}$$

where $\Delta\Sigma = \Sigma_f(\Delta q + \Delta\bar{q})$, $\Delta\vec{k}^{\,(0)} = (\Delta k_\Sigma^{(0)}, 0)^T$ and $\Delta\vec{k}^{\,(1)} = (\Delta k_\Sigma^{(1)}, \Delta k_g^{(1)})^T$ with $\Delta k_\Sigma^{(0,1)} = 2\Sigma_q \Delta k_q^{(0,1)}$ denote the inhomogeneous LO and NLO polarized photon splitting

functions into quarks and gluons [7] in (2.6) and $\Delta k_q^{(0)} = \frac{1}{2}\, 3e_q^2\, 2[2x-1]$. The 2×2 matrix $\Delta\hat{U}$ is, in complete analogy to the unpolarized case [6], expressed in terms of the usual 2×2 matrices of the polarized one– and two–loop splitting functions $\Delta\hat{P}^{(0)n}$ and $\Delta\hat{P}^{(1)n}$ which have been presented in [16] and from where also the n–moments of the coefficient functions in (2.3) and (2.4) can be obtained. The input distributions $\Delta f_{\rm had}^{\gamma(P^2),n}(\tilde{P}^2)$ in (2.16) are given by (2.10) and $L_3 \equiv \alpha_s^{(f=3)}(Q_3^2)/\alpha_s^{(3)}(\tilde{P}^2)$. For $0 \leq P^2 \leq \mu^2$ one of course has to freeze $\alpha_s^{(3)}(\tilde{P}^2)$ at $\tilde{P}^2 = \mu^2$ in order to comply with the LO and NLO boundary conditions in (2.10).

Evoluting beyond the $\overline{\rm MS}$ 'threshold' $Q_3 = m_c$, one has to take into account $f+1 = 4$ active flavors in $\alpha_s^{(f+1)}(Q^2)$ at $Q^2 \equiv Q_4^2 > m_4^2 \equiv m_c^2$ and where the results obtained in (2.15) and (2.16) at Q_3^2 serve as input for the hadronic component of the full solution in (2.14). In this way we arrive at the following general form of solutions which holds, in an obvious way, for any active number of flavors, i.e. $m_4 < Q_4 \leq m_5 \equiv m_b$ as well as for $m_5 < Q_5 \leq m_6 \equiv m_t$:

$$\begin{pmatrix} \Delta\Sigma_{p\ell}^{\gamma(P^2),n}(Q_{f+1}^2) \\ \Delta g_{p\ell}^{\gamma(P^2),n}(Q_{f+1}^2) \end{pmatrix} = \frac{4\pi}{\alpha_s^{(f+1)}(Q_{f+1}^2)} \left[1 - L_{f+1}^{1-\frac{2}{\beta_0^{(f+1)}}\Delta\hat{P}^{(0)n}}\right] \times \frac{1}{1-\frac{2}{\beta_0^{(f+1)}}\Delta\hat{P}^{(0)n}} \frac{\alpha}{2\pi\beta_0^{(f+1)}}\Delta\vec{k}^{\,(0)n} + \left[1 - L_{f+1}^{-\frac{2}{\beta_0^{(f+1)}}\Delta\hat{P}^{(0)n}}\right] \times \frac{1}{-\Delta\hat{P}^{(0)n}}\frac{\alpha}{2\pi}\left(\Delta\vec{k}^{(1)n} - \frac{\beta_1^{(f+1)}}{2\beta_0^{(f+1)}}\Delta\vec{k}^{(0)n} - \Delta\hat{U}\Delta\vec{k}^{(0)n}\right) \quad (2.17)$$

$$\left(\begin{array}{c} \Delta\Sigma_{\rm had}^{\gamma(P^2),n}(Q^2_{f+1}) \\ \Delta g_{\rm had}^{\gamma(P^2),n}(Q^2_{f+1}) \end{array} \right) = \left[L_{f+1}^{-\frac{2}{\beta_0^{(f+1)}}\Delta\hat{P}^{(0)n}} + \frac{\alpha_s^{(f+1)}(Q^2_{f+1})}{2\pi}\Delta\hat{U} L_{f+1}^{-\frac{2}{\beta_0^{(f+1)}}\Delta\hat{P}^{(0)n}} - \frac{\alpha_s^{(f+1)}(m^2_{f+1})}{2\pi} L_{f+1}^{-\frac{2}{\beta_0^{(f+1)}}\Delta\hat{P}^{(0)n}} \Delta\hat{U} \right] \times \left(\begin{array}{c} \Delta\Sigma_{p\ell}^{\gamma(P^2),n}(m^2_{f+1}) + \Delta\Sigma_{\rm had}^{\gamma(P^2),n}(m^2_{f+1}) \\ \Delta g_{p\ell}^{\gamma(P^2),n}(m^2_{f+1}) + \Delta g_{\rm had}^{\gamma(P^2),n}(m^2_{f+1}) \end{array} \right) \tag{2.18}$$

where $L_{f+1} \equiv \alpha_s^{(f+1)}(Q^2_{f+1})/\alpha_s^{(f+1)}(m^2_{f+1})$ and it should be noted that the 'pointlike' solution is always such that it vanishes, per definition, at each $Q_{f+1} = m_{f+1}$, as in (2.9) and (2.15) at $Q^2 \equiv Q_3^2 = \tilde{P}^2$. (Similar solutions have been used for calculating the parton content of unpolarized photons [6, 14]). The evolution of $\alpha_s^{(f)}(Q^2)$, corrresponding to a number of f active flavors, is obtained by exactly solving in NLO($\overline{\rm MS}$)

$$\frac{d\alpha_s^{(f)}(Q^2)}{d\ln Q^2} = -\frac{\beta_0^{(f)}}{4\pi}\left[\alpha_s^{(f)}(Q^2)\right]^2 - \frac{\beta_1^{(f)}}{16\pi^2}\left[\alpha_s^{(f)}(Q^2)\right]^3 \tag{2.19}$$

numerically [3] using $\alpha_s^{(5)}(M_Z^2) = 0.114$, rather than using the more conventional approximate solution

$$\frac{\alpha_s^{(f)}(Q^2)}{4\pi} \simeq \frac{1}{\beta_0^{(f)}\ln(Q^2/\Lambda^2)} - \frac{\beta_1^{(f)}}{(\beta_0^{(f)})^3}\frac{\ln\ln(Q^2/\Lambda^2)}{[\ln(Q^2/\Lambda^2)]^2} \tag{2.20}$$

which becomes sufficiently accurate only for $Q^2 \gtrsim m_c^2 \simeq 2$ GeV^2 with [3] $\Lambda_{\overline{\rm MS}}^{(f=4,5,6)} =$ 257, 173.4, 68.1 MeV, whereas in LO ($\beta_1 \equiv 0$) $\Lambda_{\rm LO}^{(4,5,6)} = 175, 132, 66.5$ MeV. Furthermore, $\beta_0^{(f)} = 11 - 2f/3$ and $\beta_1^{(f)} = 102 - 38f/3$. For the α_s matchings at the $\overline{\rm MS}$ 'thresholds' $Q \equiv Q_f = m_f$, i.e. $\alpha_s^{(f+1)}(m^2_{f+1}) = \alpha_s^{(f)}(m^2_{f+1})$, we have used [3] $m_c = 1.4$ GeV, $m_b = 4.5$ GeV and $m_t = 175$ GeV. On the other hand, we fix $f = 3$ in the splitting functions $\Delta P_{ij}^{(0,1)}$ in (2.17) and (2.18) for consistency since we treat the heavy quark sector $(c, b, \dots)$ by the perturbatively stable full production cross sections in fixed–order perturbation theory, i.e. $\gamma^*(Q^2)\gamma(P^2) \to c\bar{c}$ and $\gamma^*(Q^2)g^{\gamma(P^2)} \to c\bar{c}$, etc., keeping $m_c \neq 0$ as will be discussed below.

For the flavor–nonsinglet case the (matrix) solutions in eqs. (2.15)–(2.18) reduce to simple equations for $\Delta\Sigma^{\gamma(P^2)} \to \Delta q_{\rm NS}^{\gamma(P^2)}$ with $\Delta\vec{k}^{\,n} \to \Delta k_{\rm NS}^n$ [7] and $\Delta\hat{U} \to \Delta U_{\rm NS}$ expressed in terms of $\Delta P_{\rm NS}^{(0)n}$ and $\Delta P_{\rm NS}^{(1)n}$ [6, 16].

The LO results are of course entailed in the above expressions by simply dropping all the obvious higher order terms (β_1, $\Delta k^{(1)n}$, ΔU).

We shall also compare our quantitative results with the ones based on the virtual box input (2.13) as suggested in [11, 12] for $\Lambda^2 \ll P^2 \ll Q^2$. Therefore it is also useful to recall the expression for the n–moment, as defined in (2.14), of the 'box' $\Delta q_{\rm had,NLO}^{\gamma(P^2)}(x, P^2)$ in (2.13):

$$\Delta q_{\rm had,NLO}^{\gamma(P^2),n} = 3\, e_q^2\, \frac{\alpha}{2\pi} \left[\frac{2}{n} - \frac{4}{n+1} - \frac{2}{n^2} + \frac{4}{(n+1)^2} \right] . \tag{2.21}$$

All the above solutions and expressions in Mellin n–moment space can be easily converted into the desired Bjorken–x space by utilizing a numerical Mellin–inversion as described, for example, in ref. [6].

Finally, the heavy quark ($h = c, b, \dots$) contribution $g_{1,h}^{\gamma(P^2)}$ to $g_1^{\gamma(P^2)}(x, Q^2)$, as mentioned at the beginning, consists of two contributions, the 'direct' one and a 'resolved' one. The 'direct' contribution derives [17] from the polarized box diagram $\gamma^*(Q^2)\gamma \to h\bar{h}$, where the polarized virtual target photon has to be treated as a real polarized photon $\gamma \equiv \gamma(P^2 = 0)$ in order to comply with our continuity condition at $P^2 = 0$,

$$g_{1,h}^{\rm dir}(x, Q^2) = 3\, e_h^4\, \frac{\alpha}{2\pi}\, \theta(\beta^2) \left[(2x-1) \ln \frac{1+\beta}{1-\beta} + \beta(3-4x) \right] \tag{2.22}$$

where $\beta^2 = 1 - 4m_h^2/W^2 = 1 - 4m_h^2 x/(1-x)Q^2$ and $h = c, b, t$. The 'resolved' contribution derives from the polarized subprocess $\gamma^*(Q^2)g \to h\bar{h}$ and is given by [18, 19]

$$g_{1,h}^{\rm res}(x, Q^2) = \int_{y_{\rm min}}^1 \frac{dy}{y} \Delta g^{\gamma(P^2)}(y, \mu_F^2)\, \hat{g}_{1,h}^{\gamma^* g \to h\bar{h}} \left(\frac{x}{y}, Q^2 \right) \tag{2.23}$$

where $\hat{g}_{1,h}^{\gamma^* g \to h\bar{h}}(x, Q^2)$ is given by (2.22) with $e_h^4 \alpha \to e_h^2 \alpha_s(\mu_F^2)/6$, $y_{\rm min} = x(1 + 4m_h^2/Q^2)$ and $\mu_F^2 \simeq 4m_h^2$. These contributions add up to $g_{1,h}^{\gamma(P^2)} = g_{1,h}^{\rm dir} + g_{1,h}^{\rm res}$. We state these

LO results for completeness despite the fact that the NLO corrections have not yet been calculated and that the heavy quark (charm) contribution will be immaterial for our more illustrative quantitative purposes.

3 Quantitative Results

Typical LO and NLO maximal and minimal expectations for $\Delta u^{\gamma(P^2)}(x,Q^2)$ and $\Delta g^{\gamma(P^2)}(x,Q^2)$ for real and virtual polarized photons at $Q^2 = 10$ GeV^2 are shown in figs. 1 and 2 which follow from our 'maximal' input scenario in (2.10) and the 'minimal' input scenario in (2.11) which in LO is identical to the 'pointlike' solution in (2.8) as given by eqs. (2.15) and (2.17). Due to the hadronic component (2.10) in (2.8), the difference between the 'maximal' and 'minimal' scenario is of course very large for medium and small values of x for a real ($P^2 = 0$) photon, whereas this difference almost disappears already for $P^2 = 1$ GeV^2, except for $\Delta g^{\gamma(P^2)}$ at very small x in fig. 2, due to the suppression of the hadronic contribution by the dipole factor $\eta(P^2)$ in (2.10) and (2.11). Also noteworthy is the perturbative LO/NLO stability of $\Delta f^{\gamma(P^2)}(x,Q^2)$ which seems to hold in the large and small x–region as exemplified in figs. 1 and 2. Thus, for $P^2 \gtrsim 1$ GeV^2, the structure functions of longitudinally polarized virtual photons are expected to be dominated by the perturbatively uniquely calculable 'pointlike' contribution. The predicted Q^2–dependence at various fixed values of the virtuality P^2 is depicted in figs. 3 and 4. The resulting polarized structure function $g_1^{\gamma(P^2)}(x,Q^2)$ is shown in fig. 5 at some typical scales Q^2 and virtualities P^2, with the kinematical constraint $x \leq Q^2/(Q^2+P^2)$ taken into account. For illustration we also display the 'direct' heavy quark (charm) contribution according to eq. (2.22), whereas the 'resolved' contribution in (2.23) is much smaller at the scales considered.

We also compared our quantitative results with the ones based on the virtual box input (2.13), or (2.21), as studied by Sasaki and Uematsu [11, 12] for $P^2 \gg \Lambda^2$. Although we

fully confirm quantitatively their NLO results [12] for $\Delta q^{\gamma(P^2)}(x,Q^2)$ and $\Delta g^{\gamma(P^2)}(x,Q^2)$, we disagree even with their corrected ones [12] for $g_{1,\ell}^{\gamma(P^2)}(x,Q^2)$, despite the fact that we agree with their analytic expressions for $g_{1,\ell}^{\gamma(P^2)}(x,Q^2)$ as given, for example, by eq. (3.16) of ref. [11]. This discrepancy is illustrated in fig. 6 where, following [11, 12], the Q^2–evolution has been performed for fixed $f = 3$ flavors, using $\Lambda = 0.2$ GeV. (Notice that there is a trivial overall normalization difference due to the common factor of $\frac{1}{2}$ on the r.h.s. of (2.2) which has not been adopted in [11, 12]).

Next we turn to a comparison of our polarized structure functions with the rather well established unpolarized ones of real as well as of virtual photons. The fundamental positivity constraint $|\Delta\sigma| \leq \sigma$ always refers to the experimentally measurable cross sections or, in other words, to the directly measurable structure functions, i.e.

$$|g_1^{\gamma(P^2)}(x,Q^2)| \leq F_1^{\gamma(P^2)}(x,Q^2)\,, \tag{3.1}$$

implying $|A_1^{\gamma(P^2)}| \equiv |g_1^{\gamma(P^2)}/F_1^{\gamma(P^2)}| \leq 1$. Here $F_1^{\gamma(P^2)}$ (<u>not</u> $F_2^{\gamma(P^2)}$) is the spin–averaged analog of the spin–dependent $g_1^{\gamma(P^2)}$ in (2.2):

$$\begin{aligned} F_{1,\ell}^{\gamma(P^2)}(x,Q^2) \;&=\; \frac{1}{2}\sum_{q=u,d,s} e_q^2 \Big\{ q^{\gamma(P^2)}(x,Q^2) + \bar{q}^{\,\gamma(P^2)}(x,Q^2) + \frac{\alpha_s(Q^2)}{2\pi} \\ &\quad \times \Big[C_{q,1} \otimes (q+\bar{q})^{\gamma(P^2)} + 2C_{g,1} \otimes g^{\gamma(P^2)} \Big] + 2\, e_q^2\, \frac{\alpha}{2\pi}\, C_{\gamma,1}(x) \Big\} \end{aligned} \tag{3.2}$$

with $q = q_+ + q_-$ and $g = g_+ + g_-$ as compared to the spin–dependent $\Delta q = q_+ - q_-$ and $\Delta g = g_+ - g_-$ in (2.2) in terms of the positive and negative helicity densities $q_\pm$ and $g_\pm$. The NLO coefficient functions in (3.2) refer, as in (2.2), to the $\overline{\rm MS}$ factorization scheme

and are given by

$$
\begin{aligned}
C_{q,1}(x) &= C_{q,2}(x) - \frac{4}{3}\,2x \\
&= \frac{4}{3}\left[(1+x^2)\left(\frac{\ln(1-x)}{1-x}\right)_+ - \frac{3}{2}\,\frac{1}{(1-x)_+} - \frac{1+x^2}{1-x}\,\ln x + 3\right. \\
&\left. - \left(\frac{9}{2} + \frac{\pi^2}{3}\right)\delta(1-x)\right] \\
C_{g,1}(x) &= C_{g,2}(x) - \frac{1}{2}\,4x(1-x) \\
&= \frac{1}{2}\left\{\left[x^2 + (1-x)^2\right]\,\ln\,\frac{1-x}{x} + 4x(1-x) - 1\right\} \\
C_{\gamma,1}(x) &= \frac{3}{(1/2)}\,C_{g,1}(x)
\end{aligned}
\tag{3.3}
$$

which have been used in (2.11). The $\mathrm{DIS}_{\gamma,1}$ factorization scheme [10] associated with $F_{1,\ell}^{\gamma(P^2)}$ and used in the previous Section is then obtained by absorbing again the entire 'direct' $C_{\gamma,1}$ term in (3.2) into the $\overline{\mathrm{MS}}$ quark densities $q^{\gamma(P^2)} = \bar{q}^{\,\gamma(P^2)}$:

$$
\begin{aligned}
(q+\bar{q})^{\gamma(P^2)}_{\mathrm{DIS}_{\gamma,1}} &= (q+\bar{q})^{\gamma(P^2)} + e_q^2\,\frac{\alpha}{\pi}\,C_{\gamma,1}(x) \\
g^{\gamma(P^2)}_{\mathrm{DIS}_{\gamma,1}} &= g^{\gamma(P^2)}\,,
\end{aligned}
\tag{3.4}
$$

in complete analogy to the definition of the polarized $\mathrm{DIS}_{\Delta\gamma}$ factorization scheme in (2.5). Again, this redefinition of parton distributions implies that the unpolarized NLO($\overline{\mathrm{MS}}$) splitting functions $k_{q,g}^{(1)}(x)$ of the photon into quarks and gluons, appearing in the inhomogeneous NLO Q^2–evolution equations [6] for $f^{\gamma(P^2)}(x,Q^2)$, have to be transformed according to [6, 8]

$$
\begin{aligned}
k_q^{(1)}|_{\mathrm{DIS}_{\gamma,1}} &= k_q^{(1)} - e_q^2 P_{qq}^{(0)} \otimes C_{\gamma,1} \\
k_g^{(1)}|_{\mathrm{DIS}_{\gamma,1}} &= k_g^{(1)} - 2\sum_q e_q^2 P_{gq}^{(0)} \otimes C_{\gamma,1}
\end{aligned}
\tag{3.5}
$$

similarly to (2.6), where the $k_{q,g}^{(1)}(x)$ can be found, for example, in [8, 10], and $P_{qq}^{(0)} = \Delta P_{qq}^{(0)}$ and $P_{gq}^{(0)} = \frac{4}{3}\left[1+(1-x)^2\right]/x$. The NLO expression for $F_{1,\ell}^{\gamma(P^2)}$ in the $\mathrm{DIS}_{\gamma,1}$ scheme is thus given by (3.2) with $C_{\gamma,1}$ being dropped. The relevant $\mathrm{DIS}_{\gamma,1}$ parton distributions are

obtained via (2.12) from the ones in the DIS$_\gamma$ scheme [1] as derived from an analysis of the data on $F_2^\gamma(x,Q^2)$. The results at $Q^2 = 10$ GeV^2 are shown in fig. 7 for a real photon ($P^2 = 0$) and a virtual one with $P^2 = 1$ GeV^2, and are compared with the polarized structure function $g_{1,\ell}^{\gamma(P^2)}$ for our 'maximal' and 'minimal' scenario. For both cases these NLO results are in agreement [10] with the positivity constraint (3.1) which, moreover, is trivially satisfied in LO [10]. This is also illustrated in fig. 8 where, for completeness, we present the asymmetry $A_1^{\gamma(P^2)} \equiv g_{1,\ell}^{\gamma(P^2)}/F_{1,\ell}^{\gamma(P^2)}$ in LO and NLO.

The corresponding asymmetries for the (un)polarized parton distributions, $A_f^{\gamma(P^2)} \equiv \Delta f^{\gamma(P^2)}/f^{\gamma(P^2)}$, are depicted in figs. 9 and 10 in LO and NLO. In LO, where cross sections (structure functions) are directly related to parton densities, the positivity constraint (3.1) for structure functions implies

$$\Delta f^{\gamma(P^2)}(x,Q^2)| \leq f^{\gamma(P^2)}(x,Q^2) \tag{3.6}$$

which is clearly satisfied, $|A_{u,g}^{\gamma(P^2)}| \leq 1$, as shown in figs. 9 and 10 by the dashed curves. At NLO, however, a simple relation between parton distributions and cross sections no longer holds. Parton distributions are renormalization and factorization scheme dependent quantities; although universal, they are not directly observable, i.e. measurable. Hence there are NLO contributions which may violate (3.6) in specific cases [10, 20]. Such a curiosity occurs for the photonic parton distributions which, for medium to large values of x, are dominated by the photon's splitting functions $(\Delta)k_{q,g}$ appearing as inhomogeneous terms in the RG Q^2–evolution equations [6, 7, 8]. Up to NLO they are given by

$$(\Delta)k_i(x,Q^2) = \frac{\alpha}{2\pi}(\Delta)k_i^{(0)}(x) + \frac{\alpha\alpha_s(Q^2)}{(2\pi)^2}\,(\Delta)k_i^{(1)}(x) \tag{3.7}$$

where in LO $(\Delta)k_q^{(0)} = \frac{1}{2}\,3\,e_q^2\,2\left[x^2\,{}^{+}_{(-)}(1-x)^2\right]$, $(\Delta)k_g^{(0)} = 0$ and the NLO polarized (two–loop) $\Delta k_{q,g}^{(1)}$ are given in (2.7) and the unpolarized $k_{q,g}^{(1)}$ are as in (3.5). Our NLO results for $\Delta u^{\gamma(P^2)}$ and $\Delta d^{\gamma(P^2)}$ still satisfy the positivity constraint (3.6) as demonstrated by the solid curves for $A_u^{\gamma(P^2)}$ in fig. 9 since in LO $|\Delta k_q^{(0)}| \leq k_q^{(0)}$ despite the fact that the subleading NLO contributions in (3.7) in general <u>violate</u> $|\Delta k_q^{(1)}/k_q^{(1)}| \leq 1$. The NLO gluon

distributions, however, violate (3.6) because of the vanishing of the LO terms $(\Delta)k_g^{(0)} = 0$ and the now dominant NLO terms $(\Delta)k_g^{(1)}$ in (3.7) violate $|\Delta k_g^{(1)}/k_g^{(1)}| \leq 1$. This violation [10] of the NLO gluon 'positivity' is illustrated by the solid curves in fig. 10 for $A_g^{\gamma(P^2)}$ where $A_g^{\gamma(P^2)} > 1$ for $x \gtrsim 0.6$ and 0.7 – 0.85 for the 'maximal' and 'minimal' scenario, respectively.

Finally it should be mentioned that sum rules for the first ($n = 1$) moment of $g_1^{\gamma(P^2)}$ have been derived for a real ($P^2 = 0$) [21, 22] and truly virtual ($P^2 \gg \Lambda^2$) [22] polarized photon. Since our $g_{1,\ell}^{\gamma(P^2)}(x, Q^2)$ of a virtual photon in (2.2) refers to splitting and coefficient functions of on–shell partons and (real) photons, as dictated by our continuity condition at $P^2 = 0$, it is the real–photon sum rule [21, 22] that matters in our case,

$$\int_0^1 dx\, g_{1,\ell}^{\gamma(P^2)}(x, Q^2) = 0\,, \tag{3.8}$$

which derives from current conservation. Since this sum rule is maintained for all Q^2 as can be shown by inspecting [11, 12] the relevant LO and NLO evolution kernels and coefficient functions in (2.2) and (2.15) – (2.18) for $n = 1$, in particular the vanishing of the $n = 1$ moment of ΔC_γ in (2.4), it can be realized by demanding at the input scale $Q^2 = \tilde{P}^2$

$$\Delta q^{\gamma(P^2),n=1}(\tilde{P}^2) = 0\,, \tag{3.9}$$

whereas the photonic gluon distribution remains unconstrained. Our LO 'minimal' scenario in (2.11), which corresponds just to the 'pointlike' solution in (2.8), obviously satisfies (3.9) because of (2.9). On the other hand one could rather easily enforce artificially [9] the vanishing of the $n = 1$ moment of $\Delta q_{\rm had}^{\gamma(P^2)}(x, \tilde{P}^2)$ in the 'maximal' scenario (2.10) as well as of the NLO 'minimal' input in (2.11), but in view of our present complete ignorance of the hadronic component of a polarized photon we refrain from doing that. Since our quantitative speculations refer here mainly to, say, $x \gtrsim 10^{-2}$, the current conservation constraint (3.9) for the non–vanishing inputs could be accounted for by contributions from smaller x which do not affect of course the evolutions at larger x.

For completeness it should also be mentioned that for the truly virtual region $\Lambda^2 \ll P^2 \ll Q^2$, i.e. if one disregards the continuity to $P^2 = 0$, the sum rule (3.8) gets replaced by the relation [22, 11, 12]

$$\int_0^1 dx\, g_{1,\ell}^{\gamma(P^2)}(x, Q^2) = 0 - \frac{3\alpha}{2\pi} \sum_{q=u,d,s} e_q^4 + \mathcal{O}\left(\alpha\alpha_s(Q^2)\right) \tag{3.10}$$

where the LO $-\mathcal{O}(\alpha/\alpha_s)$ contribution vanishes and the finite NLO$-\mathcal{O}(\alpha)$ term derives essentially from the $n = 1$ moment of the polarized doubly–virtual 'box' $\gamma^*(Q^2)\gamma(P^2) \to q\bar{q}$ in (2.13) to $g_{1,\ell}^{\gamma(P^2)}$ in (2.2), cf. eq. (2.21). The NNLO–$\mathcal{O}(\alpha\alpha_s)$ contribution in (3.10) has been calculated as well in [22, 11, 12]. (It should be noted that different normalization and sign conventions for g_1 have been used in these latter references.) Again, this $P^2 \gg \Lambda^2$ approach could be smoothly extrapolated to $P^2 = 0$, where the sum rule (3.8) holds, by multiplying the r.h.s. of (3.10) by a form factor like [15, 22] $\zeta(P^2) = P^2/(P^2 + Q_0^2)$, as has already been discussed after eq. (2.13), where $Q_0^2 \simeq 1$ GeV^2, i.e. tpyically [22] $Q_0^2 = \mathcal{O}(m_\rho^2)$.

4 The Nonresummed QED 'Box' Contribution

An interesting question concerning the photon structure functions is where the effects due to the RG resummation actually show up. This question was studied for the unpolarized photon in [23] by comparing the contribution of the non–resummed QED 'box' cross sections for $\gamma^*(Q^2)\gamma(P^2) \to q\bar{q}$ to their QCD RG–improved counterparts.

In the present context this amounts to comparing $g_{1,\ell}^{\gamma(P^2)}(x, Q^2)_{\rm box}$, as derived from the longitudinally polarized 'box' subprocess $\vec{\gamma}^*(Q^2)\vec{\gamma}(P^2) \to q\bar{q}$, with $g_{1,\ell}^{\gamma(P^2)}(x, Q^2)$ as evaluated according to the prescriptions in Section 2. The general polarized doubly–

virtual box result for the colored three light $q = u, d, s$ quarks ($m_q = 0$) is given by [17]

$$2g_{1,\ell}^{\gamma(P^2)}(x,Q^2)_{\rm box} = 3\left(\sum_q e_q^4\right)\frac{\alpha}{\pi}\frac{1}{\bar\beta^5}\left\{(2x-1)(1-2\delta)\ln\frac{1+\bar\beta}{1-\bar\beta}\right. \tag{4.1}$$
$$\left. +\bar\beta\,[2-4x(1-2\delta)-4\delta]-8\delta x(1-x-\delta)\left[2\delta x\ln\frac{1+\bar\beta}{1-\bar\beta}-\bar\beta\right]\right\}$$

where $\delta = xP^2/Q^2$ and $\bar\beta^2 = 1-4x\,\delta$. It should be noticed that the third term proportional to $-8\delta x\ldots$ does not have any partonic interpretation since it corresponds to spin–flip transitions for each of the photons with total helicity conservation, i.e. it derives from the combination of helicity amplitudes [17] $W_{++,00} - W_{0+,-0}$ with $W_{a'b',ab}$ for the transition $ab \to a'b'$. (We have corrected for a sign misprint in eq. (E.1) of ref. [17] which results in $-\bar\beta$ in the last term in (4.1) .)

It is instructive to recall the asymptotic result of our polarized virtual ($P^2 \neq 0$) box expression derived from (4.1) in the Bjorken limit $Q^2 \gg P^2$:

$$2g_{1,\ell}^{\gamma(P^2)}(x,Q^2)_{\rm box} \simeq 3\left(\sum_q e_q^4\right)\frac{\alpha}{\pi}\left\{(2x-1)\ln\frac{Q^2}{P^2}+(2x-1)\left(\ln\frac{1}{x^2}-2\right)\right\} \tag{4.2}$$

where the appropriate 'finite' contribution has been already used in (2.13). The <u>universal</u> process independent part of this pointlike box expression proportional to $\ln Q^2/P^2$ may be used to define formally, as in the case of an unpolarized photon [23, 24], light (anti)quark distributions in the polarized photon $\gamma(P^2)$:

$$2g_{1,\ell}^{\gamma(P^2)}(x,Q^2)_{\rm box}|_{\rm univ.} \equiv \sum_{q=u,d,s} e_q^2\left[\Delta q_{\rm box}^{\gamma(P^2)}(x,Q^2)+\Delta\bar q_{\rm box}^{\gamma(P^2)}(x,Q^2)\right] \tag{4.3}$$

with

$$\Delta q_{\rm box}^{\gamma(P^2)}(x,Q^2) = \Delta\bar q\,{}_{\rm box}^{\gamma(P^2)}(x,Q^2) = 3\,e_q^2\,\frac{\alpha}{2\pi}\,(2x-1)\ln\frac{Q^2}{P^2}\,. \tag{4.4}$$

It should be noted that these naive, i.e. not QCD–resummed, box expressions do not imply a gluon component in the polarized photon, $\Delta g_{\rm box}^{\gamma(P^2)}(x,Q^2) = 0$.

Furthermore, in order to demonstrate the importance of $\mathcal{O}(P^2/Q^2)$ power corrections in the large P^2 region for photonic quark distributions, it is sometimes also useful [23] to

define, generalizing the definition (4.3), some 'effective' non–universal (anti)quark distributions as common via

$$2g_{1,\ell}^{\gamma(P^2)}(x,Q^2)_{\rm box} \equiv \sum_{q=u,d,s} e_q^2 \left[\Delta q_{\rm eff}^{\gamma(P^2)}(x,Q^2) + \Delta\bar{q}\,_{\rm eff}^{\gamma(P^2)}(x,Q^2)\right] \tag{4.5}$$

where, of course, $\Delta q_{\rm eff}^{\gamma(P^2)} = \Delta\bar{q}\,_{\rm eff}^{\gamma(P^2)}$ and the full box expression for $g_{1,\rm box}^{\gamma(P^2)}$ is given by (4.1). The full box expression implies again $\Delta g_{\rm eff}^{\gamma(P^2)}(x,Q^2) = 0$ in contrast to the QCD resummed finite gluon distribution $\Delta g^{\gamma(P^2)}(x,Q^2)$.

Our QCD–resummed total light quark distribution $\Delta\Sigma^{\gamma(P^2)}(x,Q^2) \equiv 2\sum_{q=u,d,s} \Delta q^{\gamma(P^2)}(x,Q^2)$ is compared in fig. 11 with the corresponding universal 'box' expectation according to (4.4) and with the 'effective' densities as defined in (4.5) which indicate the relevance of possible $\mathcal{O}(P^2/Q^2)$ terms. In particular in the small x region, $x \lesssim 0.3$, these latter two distributions differ significantly from the QCD resummed one. Furthermore the polarized gluon distribution, which does not exist within the box–approach, becomes comparable to $\Delta\Sigma^{\gamma(P^2)}$ below $x \lesssim 0.5$ and dominates, as ususal, in the small–x region, as in the case of an unpolarized virtual photon [23]. Thus it should be possible to distinguish between the naive box expectations and the QCD RG–improved parton distributions of a polarized photon with future dijet production measurements in polarized deep inelastic $\vec{e}\vec{p}$ experiments. Here the production rates will, in LO, be related to an effective polarized parton density [25]

$$\Delta\tilde{f}^{\gamma(P^2)}(x,Q^2) = \sum_{q=u,d,s} \left[\Delta q^{\gamma(P^2)}(x,Q^2) + \Delta\bar{q}\,^{\gamma(P^2)}(x,Q^2)\right] + \frac{11}{4}\Delta g^{\gamma(P^2)}(x,Q^2)\,, \tag{4.6}$$

with a similar relation for the proton $\Delta\tilde{f}^p(x,Q^2)$ which is assumed to be known. This equation is the polarized counterpart of a similar relation extracted from unpolarized subprocesses [26] as utilized [27] for calculating the high–p_T dijet production rates in unpolarized ep collisions.

Finally we compare in fig. 12 our QCD RG–improved predictions for the polarized structure functions $g_{1,\ell}^{\gamma(P^2)}(x,Q^2)$ for the light u,d,s quarks, to be measured in polarized

$\vec{e}^+\vec{e}^- \to e^+e^-X$ experiments, with the expectations of the naive box results in (4.1) and (4.2). Evidently, differences between these expectations may be experimentally discernible only in the small–x region, $x \lesssim 0.2$.

5 Summary

The presently unknown parton distributions, $\Delta f^{\gamma(P^2)}(x,Q^2)$, of the polarized real and virtual photon were studied in LO and NLO within the context of two extreme scenarios for their inputs at some low resolution scale. In particular it was shown how one may reasonably implement the physical requirement of their continuity at $P^2 = 0$ in the nontrivial case of a NLO analysis. The extreme 'maximal' and 'minimal' saturation scenarios are defined in NLO via eqs. (2.10) and (2.11), respectively, where the choice of the $\mathrm{DIS}_{\gamma,1}$ factorization scheme in eq. (2.10) as well as the content of eq. (2.11) were dictated by the positivity constraint $|g_1^{\gamma(P^2)}(x,Q^2)| \leq F_1^{\gamma(P^2)}(x,Q^2)$. The hadronic input in (2.10) is obtained from an analysis [1] of the unpolarized real photon data on $F_2^\gamma(x,Q^2)$ via the relation (2.12).

Finally we compare in figs. 11 and 12 the QCD resummed predictions of the 'maximal' and 'minimal' saturation models with results obtained within the framework of a simple non–resummed quark 'box' $\gamma^*(Q^2)\gamma(P^2) \to q\bar{q}$ calculation (where a gluon distribution in $\gamma(P^2)$ does not exist), expected to yield reasonable estimates in the not too small regions of x and P^2.

Acknowledgements

We thank I. Schienbein for helpful discussions concerning the calculation and results of the polarized box contribution. This work has been supported in part by the 'Bundesministerium für Bildung, Wissenschaft, Forschung und Technologie', Berlin/Bonn.

References

[1] M. Glück, E. Reya, and I. Schienbein, *Phys. Rev.* **D60** (1999) 054019; **62** (2000) 019902 (E).

[2] D. de Florian and S. Frixione, *Phys. Lett.* **B457** (1999) 236.

[3] M. Glück, E. Reya, and A. Vogt, *Eur. Phys. J.* **C5** (1998) 461.

[4] P. Ratcliffe, *Nucl. Phys.* **B223** (1983) 45.

[5] G.T. Bodwin and J. Qiu, *Phys. Rev.* **D41** (1990) 2755.

[6] M. Glück, E. Reya, and A. Vogt, *Phys. Rev.* **D45** (1992) 3986.

[7] M. Stratmann and W. Vogelsang, *Phys. Lett.* **B386** (1996) 370.

[8] M. Glück, E. Reya, and A. Vogt, *Phys. Rev.* **D48** (1993) 116.

[9] M. Glück and W. Vogelsang, *Z. Phys.* **C55** (1992) 353; **C57** (1993) 309;
M. Glück, M. Stratmann, and W. Vogelsang, *Phys. Lett.* **B337** (1994) 373.

[10] M. Glück, E. Reya, and C. Sieg, Univ. Dortmund DO–TH 2001/01 (hep–ph/0102014), Phys. Lett. B, to appear.

[11] K. Sasaki and T. Uematsu, *Phys. Rev.* **D59** (1999) 114011; *Nucl. Phys.* **B** (Proc. Suppl.) **79** (1999) 614.

[12] K. Sasaki and T. Uematsu, *Phys. Lett.* **B473** (2000) 309; Yokohama National Univ./Kyoto Univ. report YNU–HEPTh–00-102/KUCP–160 (2000) (hep–ph/0007055).

[13] T. Uematsu and T.F. Walsh, *Nucl. Phys.* **B199** (1982) 93.

[14] M. Glück, E. Reya, and M. Stratmann, *Phys. Rev.* **D51** (1995) 3220.

[15] B. Badelek, M. Krawczyk, J. Kwiecinski, and M. Stasto, Warsaw Univ. report IFT 99/13 (hep–ph/0001161).

[16] M. Glück, E. Reya, M. Stratmann, and W. Vogelsang, *Phys. Rev.* **D53** (1996) 4775.

[17] V.M. Budnev, I.F. Ginzburg, G.V. Meledin, and V.G. Serbo, *Phys. Rep.* **15** (1975) 181.

[18] A.D. Watson, *Z. Phys.* **C12** (1982) 123.

[19] M. Glück, E. Reya, and W. Vogelsang, *Nucl. Phys.* **B351** (1991) 579.

[20] G. Altarelli, S. Forte, and G. Ridolfi, *Nucl Phys.* **B534** (1998) 277.

[21] S.D. Bass, *Int. J. Mod. Phys.* **A7** (1992) 6039;
S.D. Bass, S.J. Brodsky, and I. Schmidt, *Phys. Lett.* **B437** (1998) 417;
A. Freund and L.M. Sehgal, *Phys. Lett.* **B341** (1994) 90.

[22] S. Narison, G.M. Shore, and G. Veneziano, *Nucl. Phys.* **B391** (1993) 69;
G.M. Shore and G. Veneziano, *Mod. Phys. Lett.* **A8** (1993) 373.

[23] M. Glück, E. Reya, and I. Schienbein, *Phys. Rev.* **D63** (2001) 074008.

[24] T.F. Walsh and P. Zerwas, *Phys. Lett.* **44B** (1973) 195;
C. Peterson, T.F. Walsh, and P. Zerwas, *Nucl. Phys.* **B174** (1980) 424.

[25] M. Stratmann and W. Vogelsang, contribution to the workshop on 'Polarized Protons at High Energies – Accelerator Challenges and Physics Opportunities', DESY, May 1999 (hep–ph/9907470).

[26] B.V. Combridge and C.J. Maxwell, *Nucl. Phys.* **B239** (1984) 429.

[27] C. Adloff et al., H1 Collab., *Eur. Phys. J.* **C13** (2000) 397.

Figure Captions

Fig. 1. Typical LO and NLO($\mathrm{DIS}_{\Delta\gamma}$) expectations for the parton densities of a real ($P^2 = 0$) and virtual polarized photon at a common scale of $Q^2 = 10$ GeV^2, which follow from our 'maximal' and 'minimal' input scenarios in eqs. (2.10) and (2.11), respectively.

Fig. 2. Same as in fig. 1 but plotted for a logarithmic x–scale in order to illustrate the small–x structure of the polarized distributions.

Fig. 3. The predicted Q^2–dependence of $\Delta u^{\gamma(P^2)}(x, Q^2)$ in NLO($\mathrm{DIS}_{\Delta\gamma}$) at various fixed values of the virtuality P^2 according to the 'maximal' and 'minimal' input scenarios in eqs. (2.10) and (2.11), respectively. For $P^2 = 1$ GeV^2 the results at $Q^2 = 2$ GeV^2 are, for obvious reasons, not displayed anymore.

Fig. 4. As fig. 3 but for $\Delta g^{\gamma(P^2)}(x, Q^2)$ in NLO.

Fig. 5. The resulting NLO predictions of the polarized structure function $g_{1,\ell}^{\gamma(P^2)}(x, Q^2)$ for the light u, d, s quarks as defined in (2.2), according to the 'maximal' and 'minimal' input scenarios in eqs. (2.10) and (2.11), respectively. Notice that the virtual photon structure function is kinematically constrained within $0 \leq x \leq (1 + P^2/Q^2)^{-1}$. For comparison the charm contribution at $Q^2 = 10$ GeV^2 is shown as well according to the 'direct' box expression (2.22) using $m_c = 1.4$ GeV. The 'resolved' contribution in (2.23) is marginal in the kinematic region considered.

Fig. 6. The polarized virtual photon structure function $g_{1,\ell}^{\gamma(P^2)}(x, Q^2)$ for the $f = 3$ light quark flavors at $Q^2 = 30$ GeV^2 and $P^2 = 1$ GeV$^2 \gg \Lambda^2$, where $N = (3/2)\sum_q e_q^4(\alpha/\pi)\ln(Q^2/P^2)$ with $\sum_q e_q^4 = 2/9$. Our NLO result is compared with the one presented in the second reference of ref. [12].

Fig. 7. The unpolarized and polarized structure functions $F_{1,\ell}^{\gamma(P^2)}(x, Q^2)$ and $g_{1,\ell}^{\gamma(P^2)}(x, Q^2)$ in NLO for the three light u, d, s quarks as defined in eqs. (3.2) and (2.2), respectively. $F_{1,\ell}^{\gamma(P^2)}$ has been calculated according to the analysis of ref. [1]. The results for the

polarized structure function $g_{1,\ell}^{\gamma(P^2)}$ refer to the 'maximal' and 'minimal' scenarios in eqs. (2.10) and (2.11), respectively. The Bjorken–x is kinematically constrained by $x \leq (1 + P^2/Q^2)^{-1}$.

Fig. 8. The spin asymmetries $A_1^{\gamma(P^2)}(x, Q^2) \equiv g_{1,\ell}^{\gamma(P^2)}/F_{1,\ell}^{\gamma(P^2)}$ in LO and NLO for the 'maximal' and 'minimal' scenario for $g_{1,\ell}^{\gamma(P^2)}$. The NLO results are of course directly related to the ones of fig. 7.

Fig. 9. The up–quark spin asymmetry $A_u^{\gamma(P^2)}(x, Q^2) \equiv \Delta u^{\gamma(P^2)}/u^{\gamma(P^2)}$ with $\Delta u^{\gamma(P^2)}(x, Q^2)$ being calculated according to the 'maximal' and 'minimal' scenarios in eqs. (2.10) and (2.11), respectively, and the unpolarized $u^{\gamma(P^2)}(x, Q^2)$ is calculated according to the DIS_γ results of ref. [1] using eq. (2.12). The polarized NLO distributions refer to the $\mathrm{DIS}_{\Delta\gamma}$ factorization scheme defined in (2.5), whereas the unpolarized NLO distributions are calculated in the $\mathrm{DIS}_{\gamma,1}$ scheme as defined in (3.4).

Fig. 10. As in fig. 9 but for the gluon spin asymmetry $A_g^{\gamma(P^2)}(x, Q^2) \equiv \Delta g^{\gamma(P^2)}/g^{\gamma(P^2)}$.

Fig. 11. Comparing the LO QCD–resummed total polarized light quark distribution $\Delta\Sigma^{\gamma(P^2)}(x, Q^2) \equiv 2\sum_{q=u,d,s} \Delta q^{\gamma(P^2)}$ and the polarized gluon distribution $\Delta g^{\gamma(P^2)}(x, Q^2)$ in the 'maximal' and 'minimal' scenario with the naive universal 'box' results defined in (4.4), and with the 'effective' distributions derived from (4.5). Notice that it is the quantity $(11/4)\Delta g^{\gamma(P^2)}$, which appears in the effective polarized parton density in (4.6), that will be directly accessible by future experiments.

Fig. 12. Comparing the LO– and NLO–QCD results for the polarized structure function $g_{1,\ell}^{\gamma(P^2)}(x, Q^2)$ for the light u, d, s quarks for the 'maximal' and 'minimal' input scenarios in (2.10) and (2.11) with the expectations due to the 'full box' in (4.1) and its 'asymptotic box' approximation given in (4.2) for $Q^2 \gg P^2$.

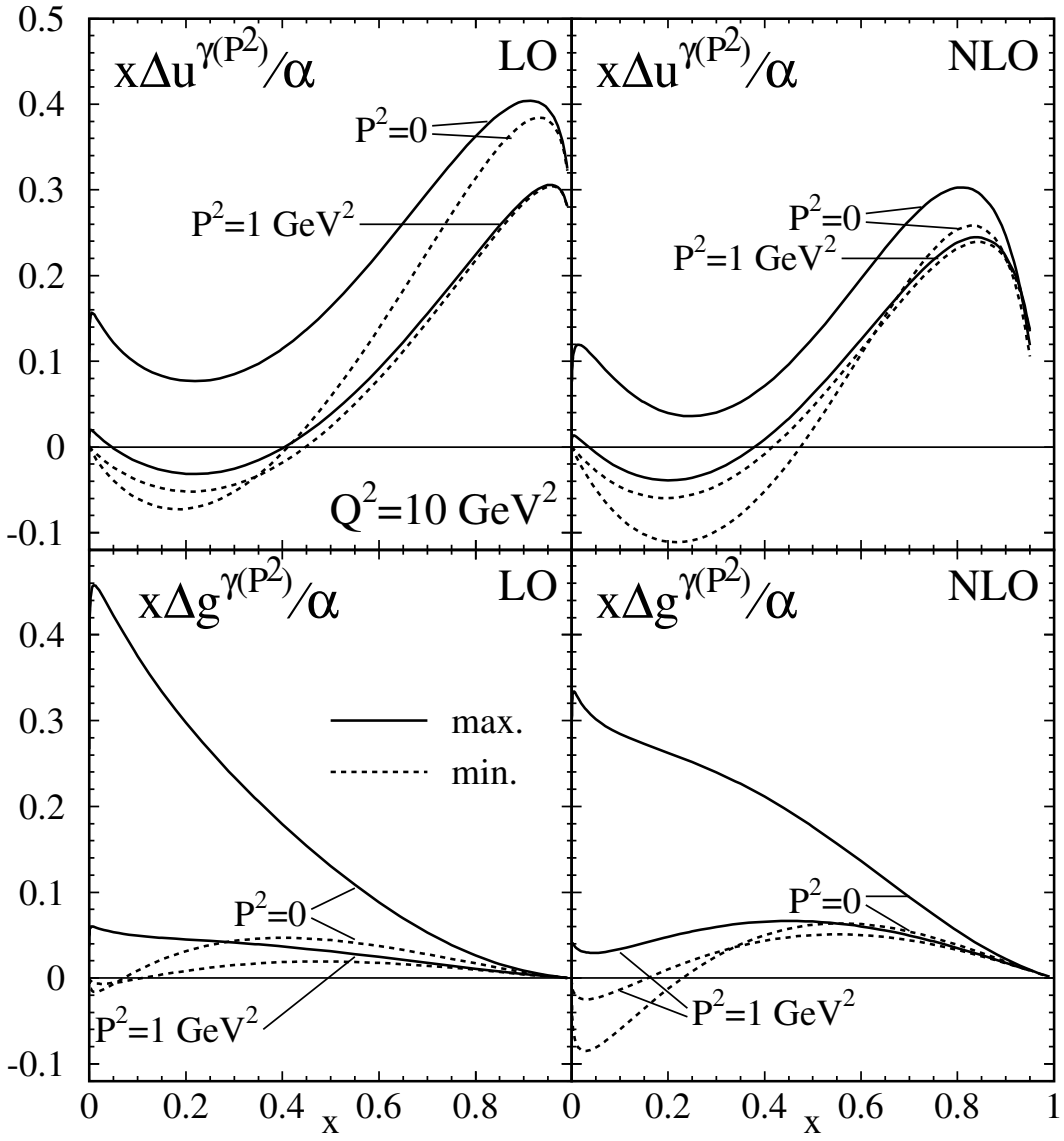

Fig. 1

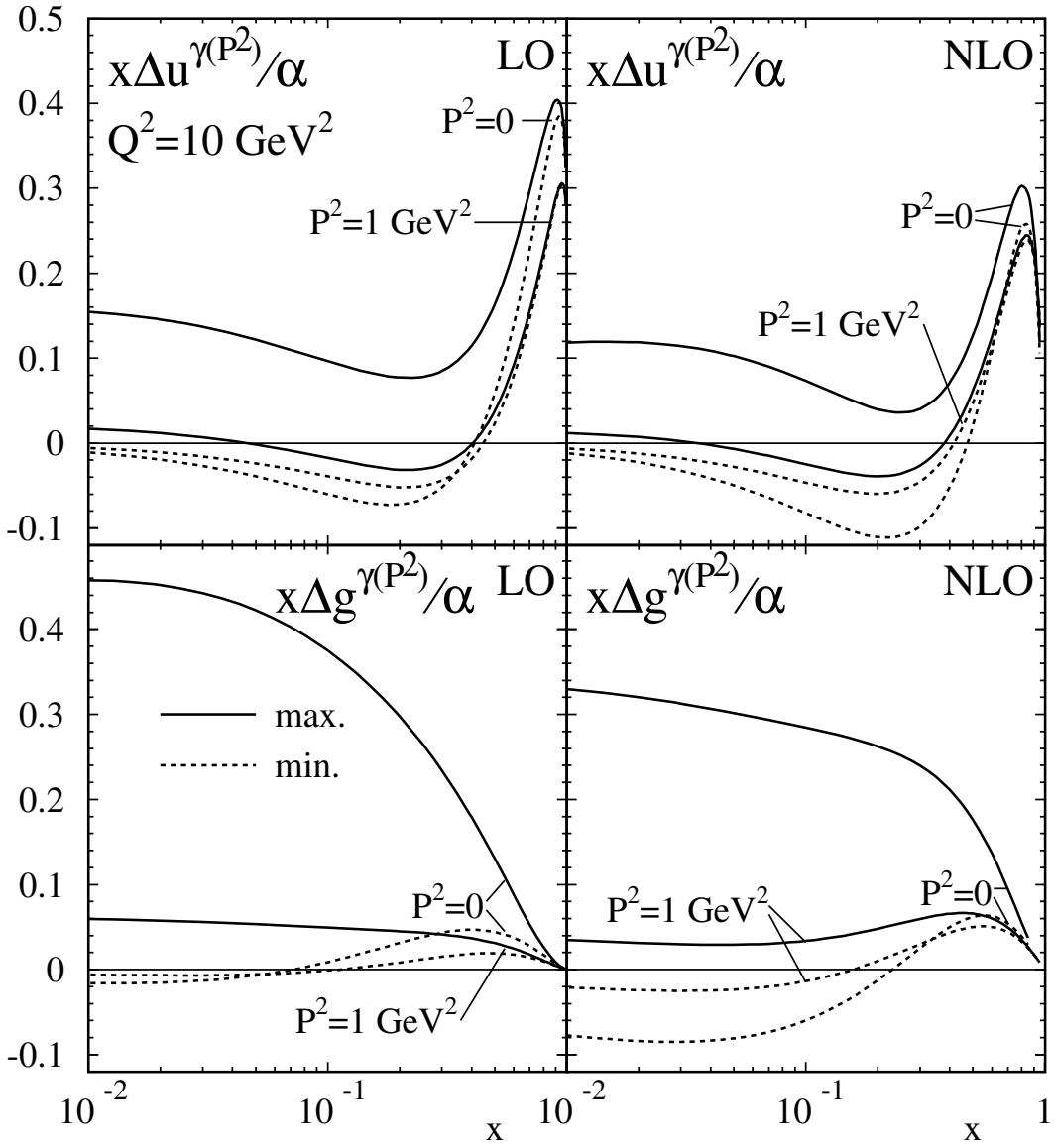
xΔu^γ(P2)/α
LO
Q2=10 GeV2
P2=0
P2=1 GeV2
xΔu^γ(P2)/α
NLO
P2=0
P2=1 GeV2
xΔg^γ(P2)/α
LO
max.
min.
P2=0
P2=1 GeV2
xΔg^γ(P2)/α
NLO
P2=1 GeV2
P2=0
0.5
0.4
0.3
0.2
0.1
0
-0.1
10 -2
10 -1
1
x

Fig. 2

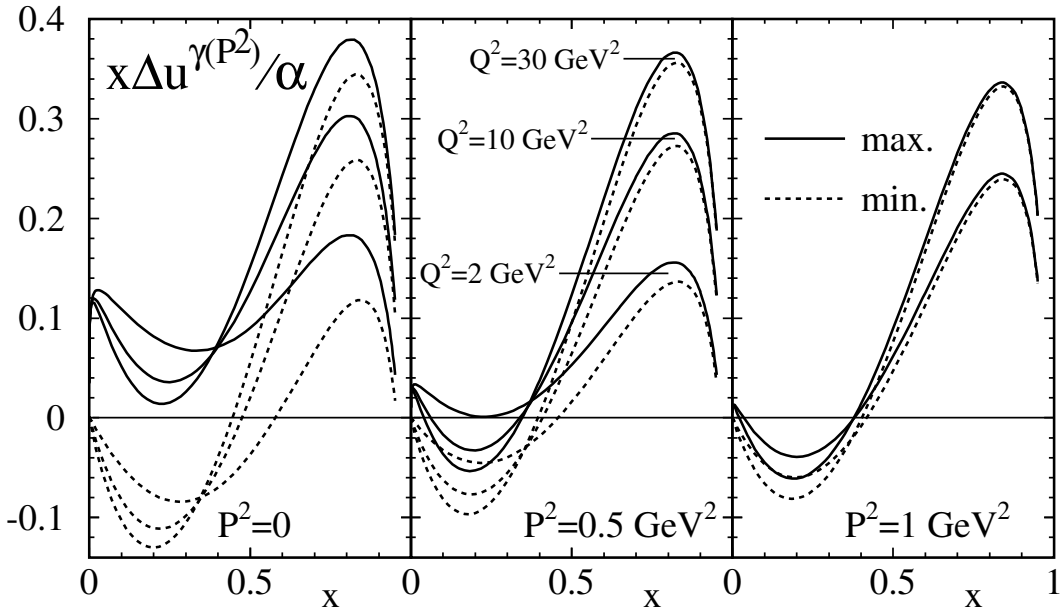
0.4
0.3
0.2
0.1
0
-0.1
$x\Delta u^{\gamma(P^2)}/\alpha$
Q^2=30 GeV^2
Q^2=10 GeV^2
Q^2=2 GeV^2
max.
min.
P^2=0
P^2=0.5 GeV^2
P^2=1 GeV^2
0
0.5
x
1

Fig. 3

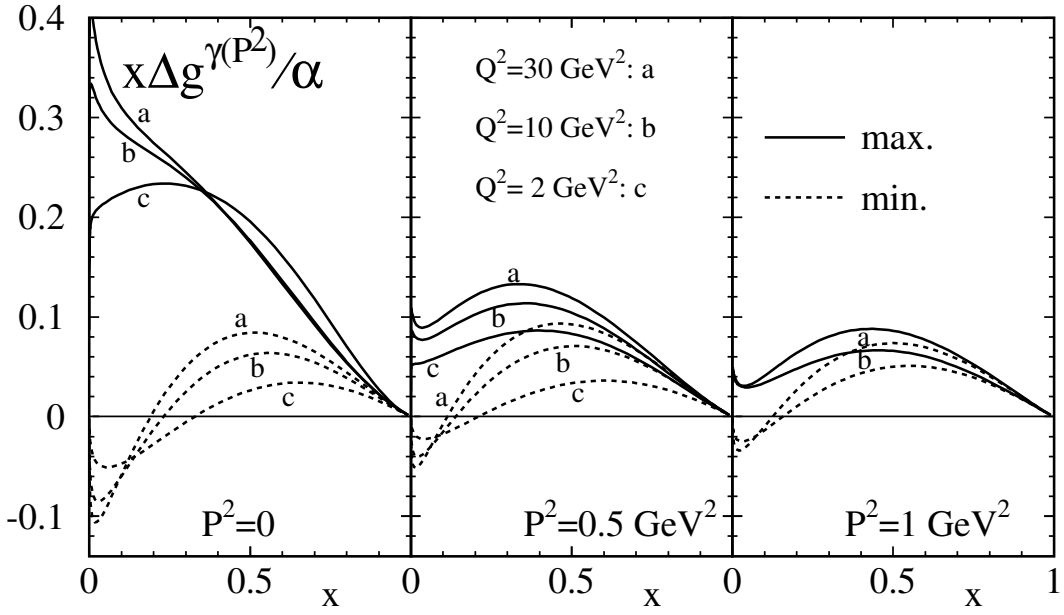
0.4
0.3
0.2
0.1
0
-0.1
$x\Delta g^{\gamma(P^2)}/\alpha$
Q^2=30 GeV^2: a
Q^2=10 GeV^2: b
Q^2= 2 GeV^2: c
max.
min.
a
b
c
P^2=0
P^2=0.5 GeV^2
P^2=1 GeV^2
0
0.5
x
1

Fig. 4

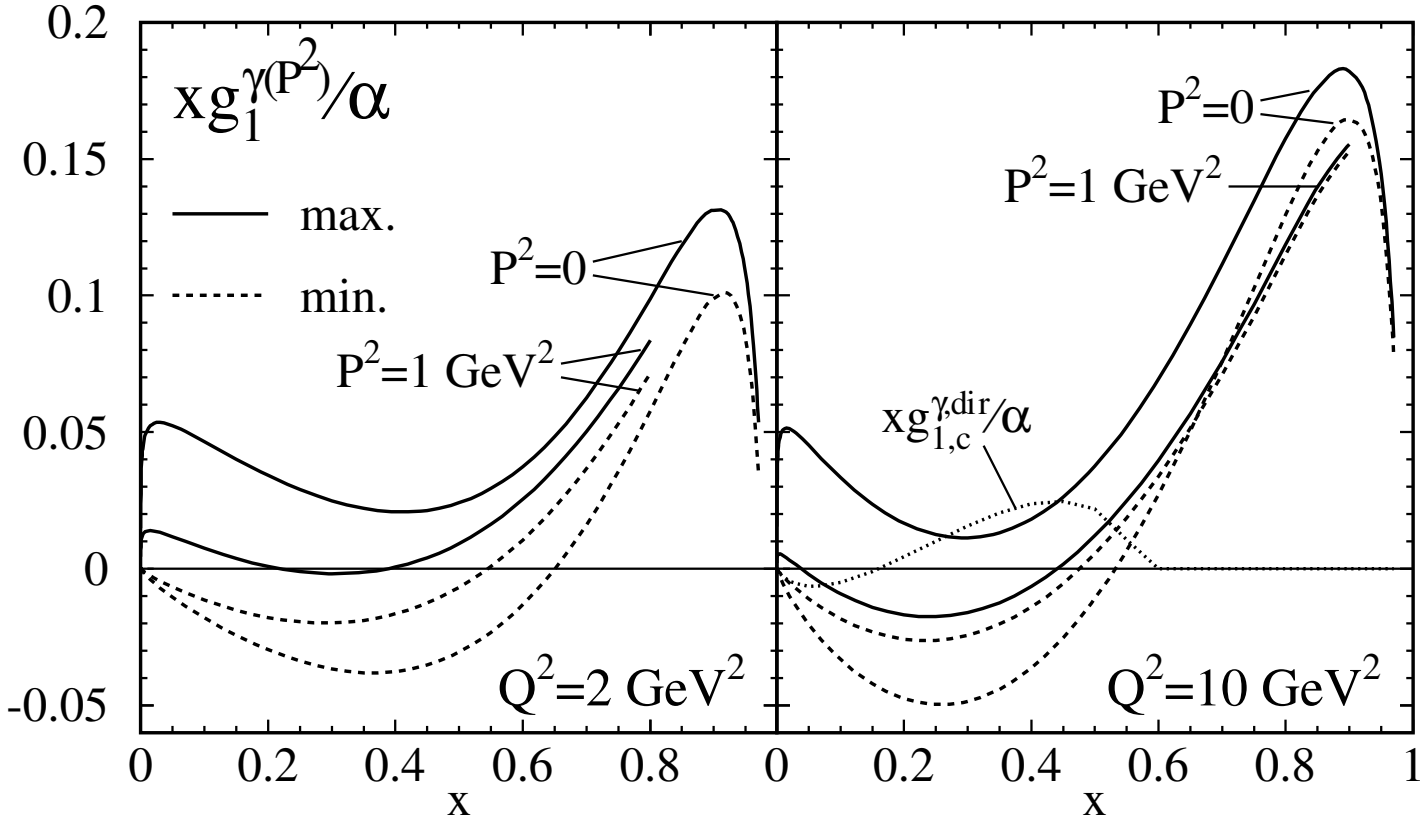
0.2
0.15
0.1
0.05
0
-0.05
$xg_1^{\gamma(P^2)}/\alpha$
max.
min.
P^2=0
P^2=1 GeV^2
Q^2=2 GeV^2
$xg_{1,c}^{\gamma,dir}/\alpha$
P^2=0
P^2=1 GeV^2
Q^2=10 GeV^2
0
0.2
0.4
0.6
0.8
1
x

Fig. 5

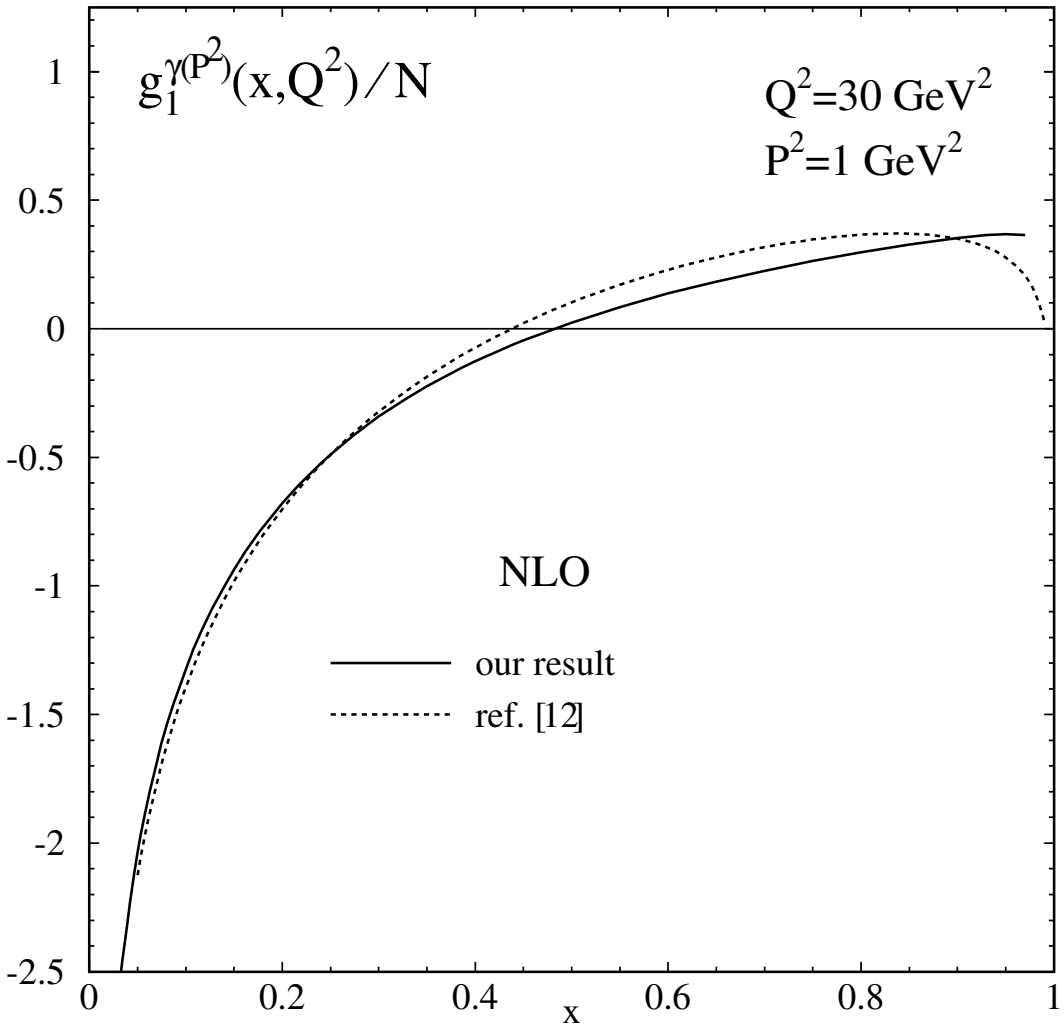
$g_1^{\gamma(P^2)}(x,Q^2)/N$
Q^2=30 GeV^2
P^2=1 GeV^2
NLO
our result
ref. [12]
1
0.5
0
-0.5
-1
-1.5
-2
-2.5
0
0.2
0.4
0.6
0.8
1
x

Fig. 6

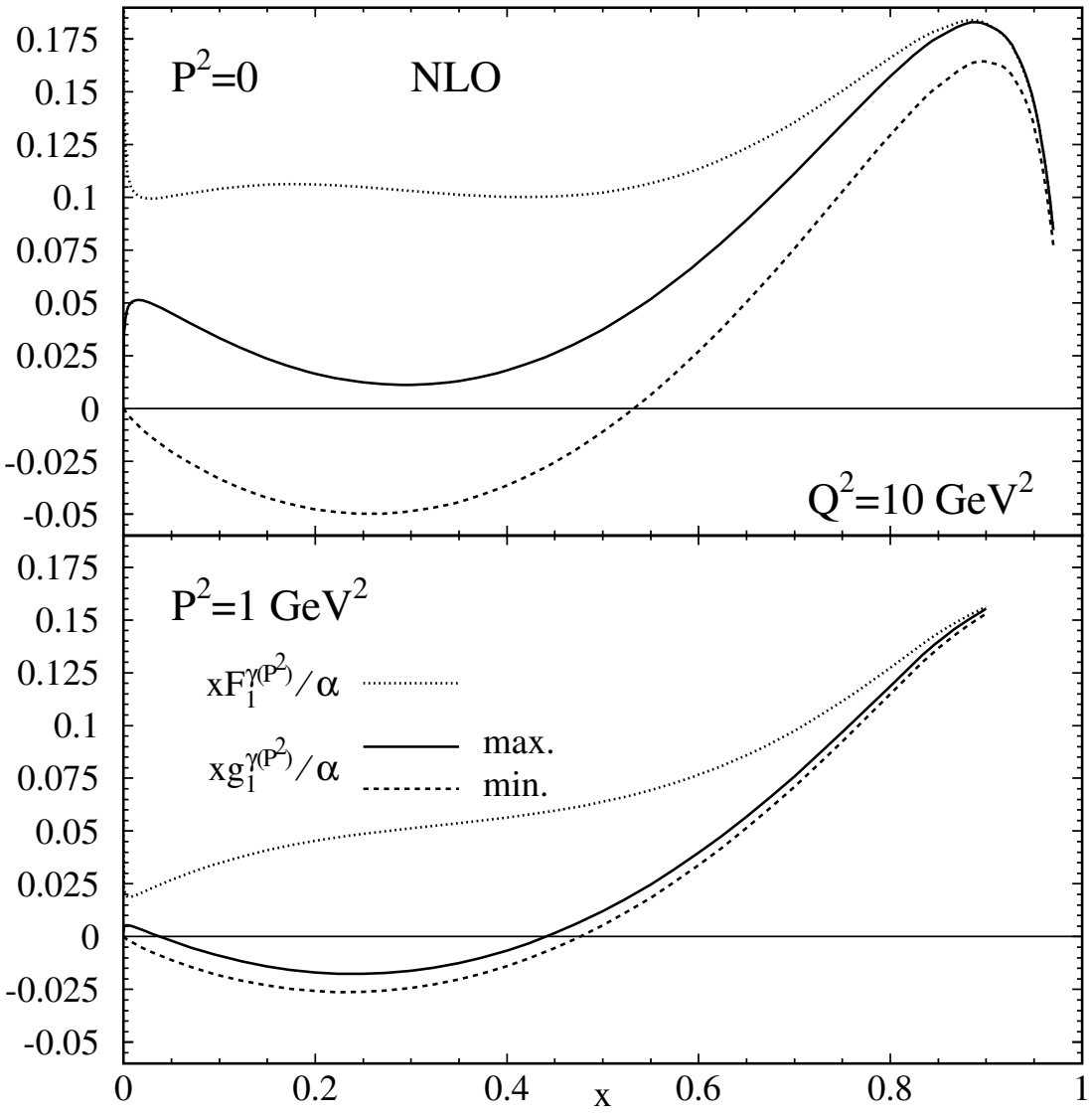
P²=0
NLO
Q²=10 GeV²
P²=1 GeV²
xF₁^γ(P²)/α
xg₁^γ(P²)/α
max.
min.
0.175
0.15
0.125
0.1
0.075
0.05
0.025
0
-0.025
-0.05
0
0.2
0.4
0.6
0.8
1
x

Fig. 7

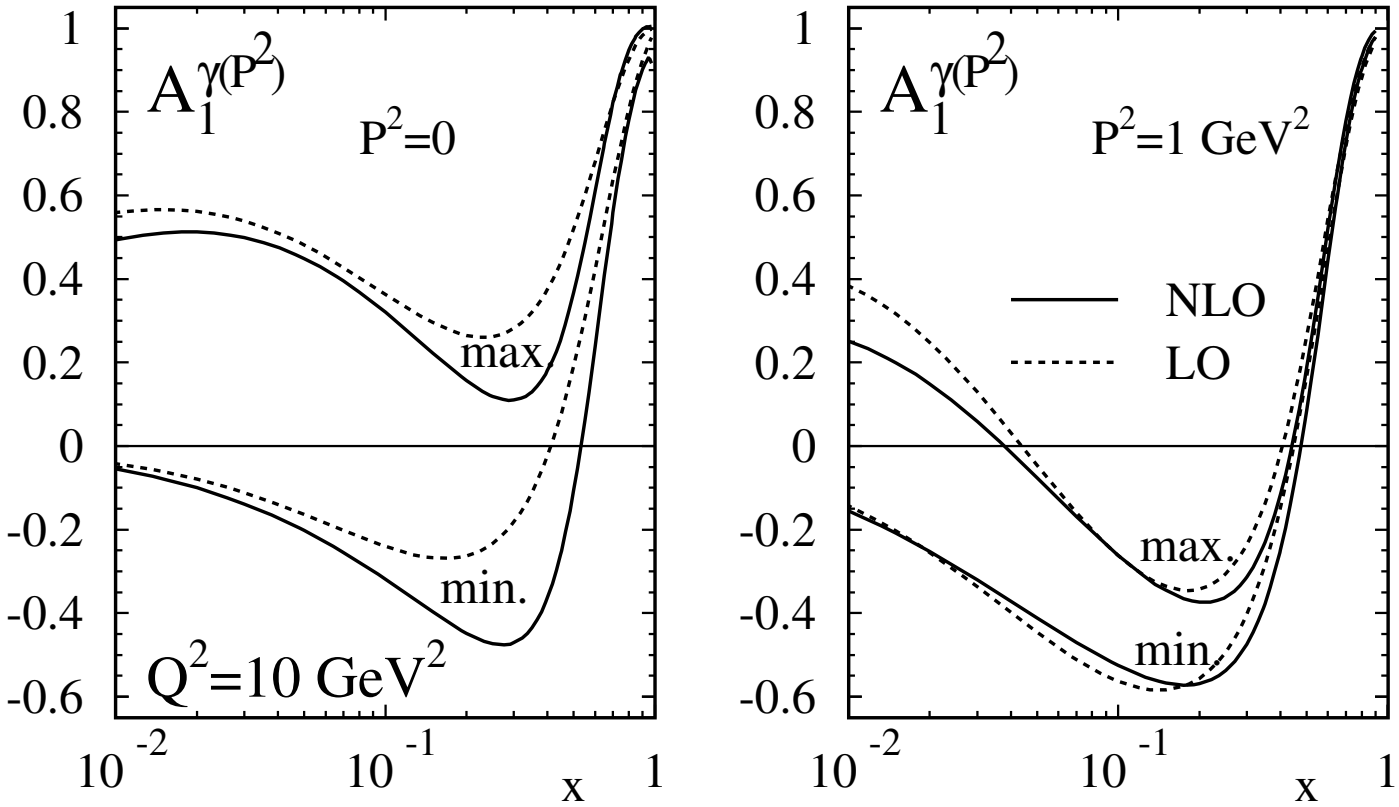
$A_1^{\gamma(P^2)}$
P^2=0
max.
min.
Q^2=10 GeV^2
P^2=1 GeV^2
NLO
LO
1
0.8
0.6
0.4
0.2
0
-0.2
-0.4
-0.6
10^{-2}
10^{-1}
x
1

Fig. 8

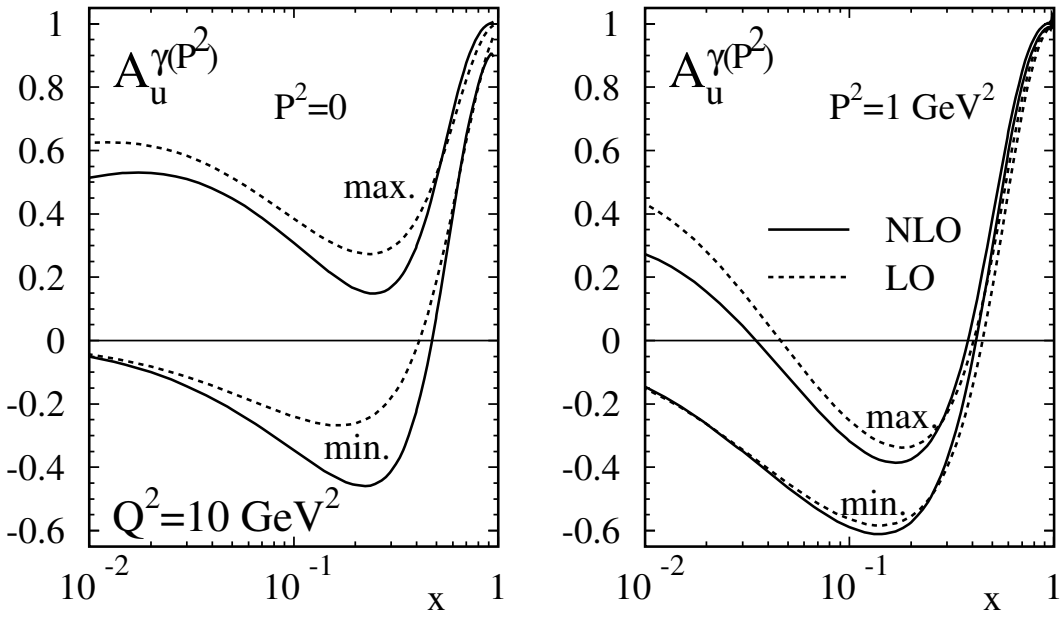
$A_u^{\gamma(P^2)}$
P^2=0
max.
min.
Q^2=10 GeV^2
P^2=1 GeV^2
NLO
LO
x

Fig. 9

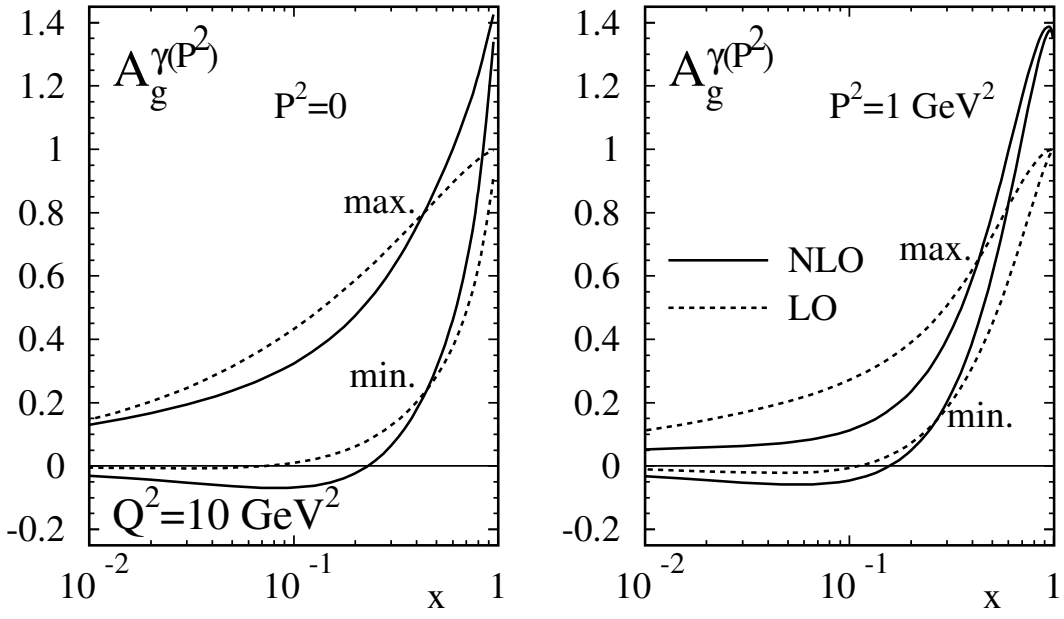
$A_g^{\gamma(P^2)}$
P^2=0
max.
min.
Q^2=10 GeV^2
P^2=1 GeV^2
NLO
LO
x

Fig. 10

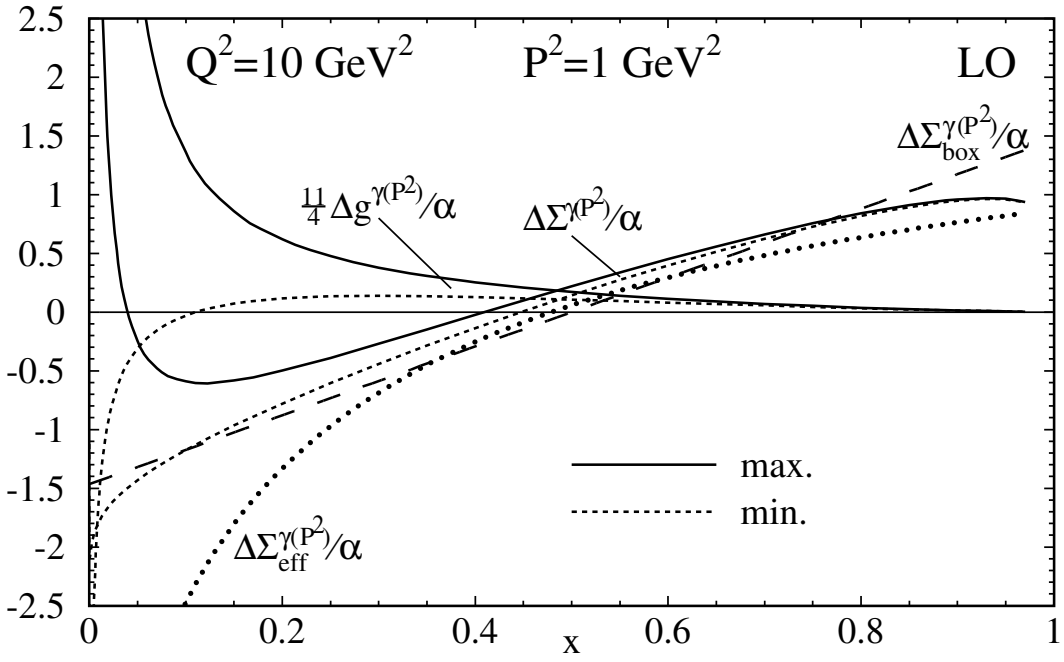
Q^2=10 GeV^2
P^2=1 GeV^2
LO
$\Delta\Sigma^{\gamma(P^2)}_{box}/\alpha$
$\frac{11}{4}\Delta g^{\gamma(P^2)}/\alpha$
$\Delta\Sigma^{\gamma(P^2)}/\alpha$
max.
min.
$\Delta\Sigma^{\gamma(P^2)}_{eff}/\alpha$
x

Fig. 11

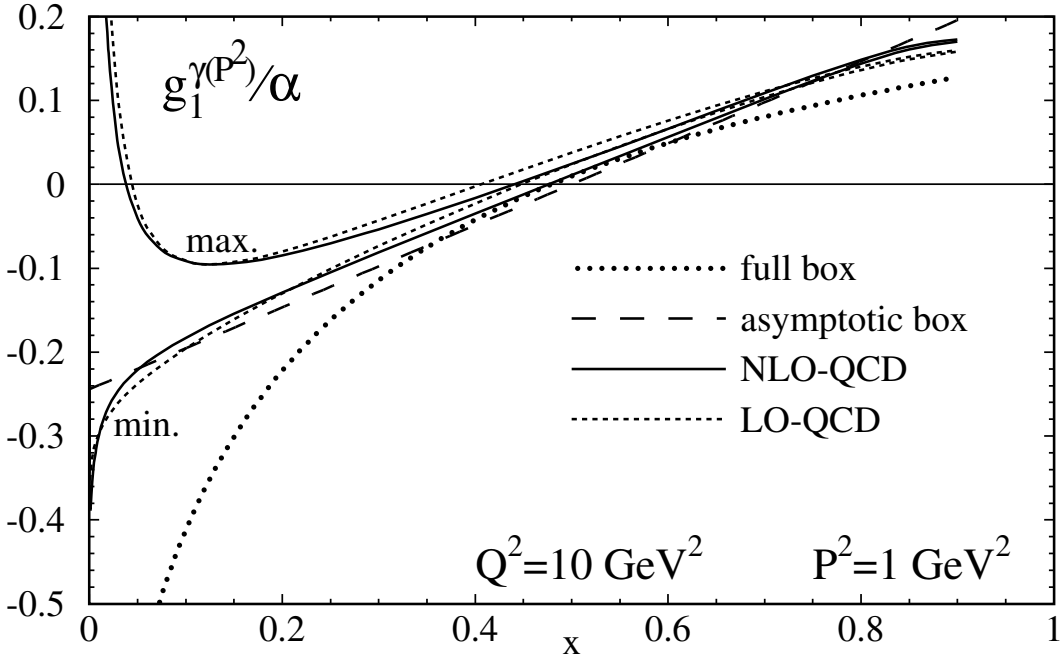
$g_1^{\gamma(P^2)}/\alpha$
max.
min.
full box
asymptotic box
NLO-QCD
LO-QCD
Q^2=10 GeV^2
P^2=1 GeV^2
x

Fig. 12